USGS Science Strategy to Support U.S. Fish and Wildlife Service Polar Bear Listing Decision

Predicting the Future Distribution of Polar Bear Habitat in the Polar Basin from Resource Selection Functions Applied to 21st Century General Circulation Model Projections of Sea Ice

By George M. Durner[1], David C. Douglas[2], Ryan M. Nielson[3], Steven C. Amstrup[1], and Trent L. McDonald[3]

Administrative Report

U.S. Department of the Interior
U.S. Geological Survey

U.S. Department of the Interior
DIRK KEMPTHORNE, Secretary

U.S. Geological Survey
Mark D. Myers, Director

U.S. Geological Survey, Reston, Virginia: 2007

Author affiliations:

[1]U.S. Geological Survey, Alaska Science Center, Anchorage
[2]U.S. Geological Survey, Alaska Science Center, Juneau
[3]Western EcoSystems Technology, Inc., Laramie, Wyoming

Contents

Figures

Tables

Abbreviations, Acronyms, and Symbols

Abbreviations, Acronyms, and Symbols	Meaning
20C3M	20th Century Experiment
ADCLS	Argos Data Collection and Location System
AIC	Akaike's Information Criterion
AR-4	IPCC Fourth Assessment Report
BIC	Bayesian Information Criterion
CCSM3	NCAR model
CMIP3	WCRP Coupled Model Intercomparison Project, Phase 3
GCM	General circulation models
GPS	Global Positioning System
Had1SST	Hadley Center sea ice and surface temperature data set
IBCAO	International Bathymetric Chart of the Arctic Ocean
IPCC	Intergovernmental Panel on Climate Change
IUCN	International Union for Conservation of Nature and Natural Resources
NASA	National Aeronautics and Space Administration
NCAR	National Center for Atmospheric Research
PBSG	IUCN Polar Bear Specialist Group
PMW	Passive microwave
PTT	Platform transmitter terminal
RSF	Resource selection functions
SRES	IPCC Special Report on Emission Scenarios
TIN	Triangular irregular network
USGS	U.S. Geological Survey
WCRP	World Climate Research Programme

Predicting the Future Distribution of Polar Bear Habitat in the Polar Basin from Resource Selection Functions Applied to 21st Century General Circulation Model Projections of Sea Ice

By George M. Durner, David C. Douglas, Ryan M. Nielson, Steven C. Amstrup, and Trent L. McDonald

Abstract

Predictions of polar bear (*Ursus maritimus*) habitat distribution in the Arctic polar basin during the 21st century were developed to help understand the likely consequences of anticipated sea ice reductions on polar bear populations. We used location data from satellite-collared polar bears and environmental data (e.g., bathymetry, coastlines, and sea ice) collected between1985–1995 to build habitat-use models called Resource Selection Functions (RSF). The RSFs described habitats polar bears preferred in each of four seasons: summer (ice minimum), autumn (growth), winter (ice maximum) and spring (melt). When applied to the model source data and to independent data (1996–2006), the RSFs consistently identified habitats most frequently used by polar bears. We applied the RSFs to monthly maps of 21st century sea ice concentration predicted by 10 general circulation models (GCM) described in the International Panel of Climate Change Fourth Assessment Report. The 10 GCMs we used had high concordance between their simulations of 20th century summer sea ice extent and the actual ice extent derived from passive microwave satellite observations. Predictions of the amount and rate of change in polar bear habitat varied among GCMs, but all GCMs predicted net habitat losses in the polar basin during the 21st century. Projected losses in the highest-valued RSF habitat (optimal habitat) were greatest in the peripheral seas of the polar basin, especially the Chukchi Sea and Barents Sea. Losses were least in high-latitude regions where RSFs predicted an initial increase in optimal habitat followed by a modest decline. The largest seasonal reductions in habitat were predicted for spring and summer. Average area of optimal polar bear habitat during summer in the polar basin declined from an observed 1.0 million km^2 in 1985–1995 (baseline) to a projected multi-model average of 0.58 million km^2 in 2045–2054 (-42% change), 0.36 million km^2 in 2070–2079 (-64% change), and 0.32 million km^2 in 2090–2099 (-68% change). After summer melt, most regions of the polar basin were projected to refreeze throughout the 21st century, so winter losses of polar bear habitat were more modest; from 1.7 million km^2 in 1985–1995 to 1.4 million km^2 in 2090–2099 (-17% change). Simulated and projected rates of habitat loss during the late-20th and early-21st centuries by many GCMs tended to be less than observed rates of loss during the past 2 decades. Hence, we consider habitat losses based on GCM multi-model averages to be conservative. Although less available habitat will likely reduce polar bear populations, exact relationships between habitat losses and population demographics remain unknown. Density effects may become important because polar bears that make long distance annual migrations from traditional winter ranges to remnant high-latitude summer sea ice will enter regions already occupied by polar bears. Declines and large seasonal swings in habitat

availability and distribution may impose greater impacts on pregnant females seeking denning habitat or leaving dens with cubs than on other sex and age groups. Despite annual replenishment of most winter habitats, large retreats of summer habitat may ultimately preclude bears from seasonally returning to their traditional winter ranges.

Introduction

The U.S. Fish and Wildlife Service proposed listing the polar bear (*Ursus maritimus*) as a threatened species under the Endangered Species Act in January 2007 (USFWS 2007). To help inform their final decision, they requested that the U.S. Geological Survey (USGS) conduct additional analyses about polar bear populations and their sea ice habitats. Between February and August 2007, USGS and collaborators developed nine reports targeting specific questions considered especially informative to the final decision. This is one of the nine reports. This report focuses on the expected distribution of polar bear habitat in the 21st century in the polar basin region. We quantified relationships between observed polar bear distributions and sea ice conditions (and other constant environmental factors such as bathymetry and distance to shore) by constructing resource selection functions (RSF), then extrapolating the RSF models using forecasts of future sea ice distribution. This analysis allowed us to evaluate trends in the amount, quality, and location of polar bear sea ice habitat into the 21st century.

The extent and composition of Arctic sea ice is pivotal for the survival of wild populations of polar bears (Amstrup 2003). Polar bears evolved during the late Pleistocene to fill an otherwise empty niche as highly specialized surface-based predators on sea-ice dependent phocid seals, primarily ringed seals (*Phoca hispida*) and bearded seals (*Erignathus barbatus*; Stirling and Archibald 1977). The sea ice allows polar bears to exploit the productive marine environment by providing a platform from which they can hunt seals. Polar bears also evolved in an environment that, with the exception of humans in near shore areas, has been largely free of competitors and predators. This isolation in a relatively persistent Arctic climate has allowed polar bears to flourish on the Arctic sea ice.

There are currently estimated to be approximately 25,000 polar bears (Aars et al. 2006) distributed over a maximum of 1.5×10^7 km^2 of northern hemisphere sea ice (average 1979–2006 winter estimate; National Snow and Ice Data Center, Boulder, CO). Polar bears are not distributed uniformly on Arctic sea ice but instead appear to select specific sea ice features (Stirling et al. 1993; Arthur et al. 1996; Ferguson et al. 2000; Mauritzen et al. 2001; Durner et al. 2004; Durner et al. 2006). Sea ice over and near the continental shelf appears to be preferred habitat (Derocher et al. 2004, Durner et al. 2004), likely because of higher biological productivity (Dunton et al. 2005), and greater accessibility to prey in near shore shear zones and polynyas (Stirling 1997), compared to deep-water regions in the central polar basin. However, in addition to selecting habitats based on prey availability, polar bears may also select areas of relatively high sea ice concentration to attain safety during storms (Mauritzen et al. 2003a).

Nineteen polar bear subpopulation units are currently recognized by the International Union for the Conservation of Nature and Natural Resources (IUCN) Polar Bear Specialist Group (PBSG; Aars et al. 2006; Fig. 1). The 19 IUCN units may be grouped into 3 "ecoregions" based on seasonal differences in sea ice patterns, the proximity and dispersion of land masses, and by the behavior of polar bears that occupy each region (Amstrup et al. 2007). Following Amstrup et al. (2007), these ecoregions include: 1) a region of seasonal sea ice (IUCN units Baffin Bay, Davis Strait, Foxe Basin, Southern Hudson Bay and Western Hudson Bay); 2) the islands and channels within the Canadian Arctic

archipelago (IUCN units Gulf of Boothia, Kane Basin, Lancaster Sound, M'Clintock Channel, Norwegian Bay and Viscount Melville); and 3) the pelagic region of the polar basin, which contains open ocean sea ice in most of its extent throughout the year (IUCN units Arctic Basin, Barents Sea, Chukchi Sea, East Greenland Sea, Kara Sea, Laptev Sea, Northern Beaufort Sea and Southern Beaufort Sea; Fig. 1). The estimated number of polar bears is 7700 in the seasonal ice region, 5000 in the archipelago region, and 11,900 in the pelagic region (Amstrup et al. 2007).

The pelagic ecoregion can be divided in 2 sub-regions (Fig. 1) that are characterized by annual patterns of sea ice formation, movement, and ablation (Rigor et al. 2002, Rigor et al. 2004, Amstrup et al. 2007, Maslanik et al. 2007, Meier et al. 2007, Ogi and Wallace 2007). This includes peripheral regions of the polar basin where annual ice is formed and exported to other regions (divergent sea ice; Fig. 1), which we term as the "Alaska-Eurasia" region (IUCN units Barents Sea, Chukchi Sea, Kara Sea, Laptev Sea and Southern Beaufort Sea). The polar basin also includes a region of convergent sea ice (ice that largely originates from the Alaska-Eurasia region), which we term as the "Canada-Greenland" region (IUCN units Arctic Basin, East Greenland Sea, Northern Beaufort Sea).

Contemporary observations and state-of-the-art models point to a warming global climate, with some of the most accelerated changes in polar regions. In the past 30 years, average world surface temperatures have increased 0.2°C per decade, but parts of the Arctic have experienced 10-fold the average warming (Hansen et al. 2006). Since the late-1970s there have been major reductions in summer (multiyear) sea ice extent (Meier 2007), decreases in ice age (Rigor and Wallace 2004, Belchansky et al. 2005) and thickness (Rothrock et al. 1999, Tucker et al. 2001), and increases in length of the summer melt period (Belchansky et al. 2004, Stroeve et al. 2005). Recent observations further indicate that winter ice extent has started to decline (Comiso 2006). Hence, empirical evidence establishes that the environment on which polar bears depend for their survival has already changed substantially. Of particular concern are the longer melt seasons and reduced summer ice extent that force more polar bears into habitats where their hunting success is likely compromised (Derocher et al. 2004, Stirling and Parkinson 2006).

Most coupled ocean-atmosphere general circulation models (GCM) forecast continued reductions in ice extent and multiyear ice throughout the 21st century (Holland et al. 2006, Zhang and Walsh 2006). The projections of 21st century sea ice declines, however, appear to be conservative because the observed rate of sea ice loss to-date is greater than that estimated by most IPCC AR-4 GCMs (sensu "faster than forecasted", Stroeve et al. 2007).

Habitat loss has been implicated as the greatest threat to the survival of most species (Wilcove et al. 1998). Extinction theory suggests that the most vulnerable species are those that are specialized (Davies et al. 2004), long-lived with long generation times and low reproductive output (Bodmer et al. 1997), and are carnivores with a large geographic extent and low population densities (Viranta 2003). Because of their specialized habitats and life history constraints (Amstrup 2003), polar bears have many qualities that make their populations susceptible to the potential negative aspects of sea ice loss resulting from climate change.

Without sea ice, polar bears lose their ability to interface with the productive marine environment. Increases in duration of the summer season, when polar bears are restricted to land or forced over relatively unproductive Arctic waters, may reduce individual survival and ultimately reduce populations (Derocher et al. 2004). Phocid seals do not necessarily use sea ice during summer and so may be inaccessible to polar bears during extensive summer melting (Harwood and Stirling 1992).

Unusual movements, such as long distance swims to reach pack ice or land, place polar bears in potentially hazardous environments (Monnett and Gleason 2006).

A declining sea ice environment may impose nutritional stress on polar bears and cause them to resort to novel food sources including cannibalism (Amstrup et al. 2006) and anthropogenic foods (Stirling and Parkinson 2006). In an environment of declining sea ice, polar bears must often endure longer periods with little or no hunting opportunities, the effect of which has been linked to a decline in at least one population –Western Hudson Bay, located at the southern end of the species' range (Stirling and Parkinson 2006, Regehr et al. 2007).

In this report, we use location data from satellite-collared polar bears and environmental data (e.g., sea ice concentration, bathymetry, etc.) to develop resource selection functions (RSF; Manly et al. 2002) of habitat selection by polar bears. We use the RSFs to empirically model the late-20th century distribution of preferred polar bear habitat in the polar basin. We then extrapolate those RSFs to GCM predictions of 21st century sea ice distribution to forecast the future extent and distribution of polar bear habitat.

Methods

Study area

Our study area was the pelagic ecoregion of the Arctic Ocean and its peripheral seas, including the Alaska-Eurasia and Canada-Greenland subregions. In addition to the 8 IUCN polar bear subpopulation units identified within the pelagic ecoregion by the PBSG (Aars et al. 2006), we identified another unit which we named Queen Elizabeth (Fig. 1). The Queen Elizabeth unit was carved from the largely pelagic Arctic Basin IUCN unit to include the continental shelf region extending north from the Queen Elizabeth Islands and NE Greenland.

Polar bear location data

We used location data from satellite radio collars deployed on adult female polar bears captured in several regions of the polar basin, 1985–2006. The majority of data came from polar bears marked in the Chukchi and Beaufort seas by the USGS. Data also came from polar bears marked in Canadian regions of the Beaufort Sea (1992–1995) and Viscount Melville Sound (1989–1993) by the Canadian Wildlife Service, the Barents Sea (1988–1999) by the Norwegian Polar Institute, and in the East Greenland Sea (1993–1998) by the Danish Institute of Natural Resources. Polar bears were captured with standard animal immobilization techniques (Stirling et al. 1989) during March – June (all jurisdictions), and during October – November (USGS only).

The majority of bears were equipped with satellite radio collars (platform transmitter terminal, or PTT; Telonics, Inc., Mesa, AZ) that transmitted signals from which locations were calculated by the Argos Data Collection and Location System (ADCLS; Fancy et al. 1988). Most PTTs transmitted for 4–8 hours every 1–7 days (duty cycle). Several locations were typically obtained during each duty cycle. For analysis we used standard-quality locations only (Argos Location Classes 1, 2 or 3) which are generally accurate to within 1.2 km (Keating et al. 1991).

In 2004–2006, the majority of satellite radio-collars deployed by USGS in the Beaufort Sea used Global Positioning System (GPS; Telonics, Mesa, AZ) technology for location determination. Locations calculated by a GPS receiver within the collar were then transmitted to USGS via ADCLS. Both PTTs and GPS satellite-radio collars typically collected several high quality locations per duty cycle.

For both ADCLS and GPS locations, we randomly selected at most one location per bear per day. From these, we retained only those locations that were within our study area. Pregnant polar bears occupy maternal dens

between October and April (Amstrup and Gardner 1994). To eliminate the potential bias resulting from denning polar bears, we used temperature and activity sensor data (Fischbach et al. 2007) to identify and remove all locations during the time that they were known to be in dens. We were interested in the habitat choice that a bear made as it moved between two consecutive locations, hence we used pairs of consecutive locations that were separated by 4–8 days (Ferguson et al. 2000).

For analysis, we divided the polar bear location data into 2 decadal time periods based on differences in collaring effort and sea ice conditions: (1) 1985–1995, and (2) 1996–2006. We used 1985–1995 as the baseline period to determine polar bear selection indices because during this early period of our studies year-round polar bear movements were less restricted than during the more recent years of reduced sea ice extent. Sea ice conditions markedly changed post-1995 (Ogi and Wallace 2007). Also, the 1985–1995 tracking data better represented all polar bear populations throughout the Arctic basin (Table 3). After 1995, the proportion of polar bear location data in the Chukchi, Laptev and Kara seas was greatly reduced, while the proportion from the southern Beaufort Sea essentially doubled (60.7% after 1995 vs. 30.9% prior to 1996). We therefore postulated that RSF models derived from 1985–1995 data would more accurately represent resource selection across the study area under historical ice regimes than would models developed from more recent data. And, building the RSF models from the 1985–1995 data also allowed us to examine the degree of change in polar bear habitats between the 2 time periods – using strictly observational data.

Observational habitat data

Estimates of monthly sea ice concentration derived from satellite passive microwave (PMW) brightness temperatures using the NASA Team Algorithm (Cavalieri et al. 1990) were obtained from the National Snow and Ice Data Center (Boulder, CO., USA, *http://nsidc.org/data/nsidc-0051.html*). The PMW sea ice concentration data were disseminated in raster format with a 25 km × 25 km pixel size in polar stereographic projection. The polar-orbiting PMW sensors do not view a small region around the North Pole due to an inclination in the satellite orbits. We set missing data within this "pole hole" to 100% ice concentration, since this high-latitude region has been almost completely ice covered during the entire observational period.

We used the International Bathymetric Chart of the Arctic Ocean (IBCAO, Jakobsson et al. 2000) for extracting estimates of ocean depth. The IBCAO data were distributed in a polar stereographic projection grid with 2.5 km pixel resolution. We re-sampled the native bathymetry grid to 25 km pixel resolution (identical to PMW) by averaging depth within the boundaries of each PMW pixel.

General circulation model data

We extrapolated the RSF models using monthly sea ice concentration grids from 10 Intergovernmental Panel of Climate Change (IPCC) Fourth Assessment Report (AR-4) fully-coupled GCM models (Table 1). These included hindcast ice estimates from the 20th Century Experiment (20C3M, forced by observed natural and anthropogenic environmental factors) and projection estimates for the 21st century based on a 'business as usual' greenhouse gas forcing SRES-A1B scenario (Special Report on Emission Scenarios). For one GCM (CCSM3), we also extrapolated the RSF models using 21st century ice projections based on the SRES-B1 scenario, which reflects a more gradual increase in greenhouse gas forcing ($CO_2 \approx 550$ ppm by 2100) compared to the SRES-A1B scenario ($CO_2 \approx 720$ ppm by 2100). We obtained all GCM data from the World Climate Research Programme's (WCRP's) Coupled Model Intercomparison

Project phase 3 (CMIP3) multi-model dataset (*https://esg.llnl.gov:8443*), except CCSM3 which we obtained directly from the National Center for Atmospheric Research in its native CCSM grid format (D. Bailey and M. Holland, NCAR, pers. comm.). We obtained and analyzed one ensemble member (run-1) for each GCM, except CCSM3 for which we obtained 8 runs.

We selected the 10 GCMs (Table 1) from a larger group of 20 based on an analysis of concordance (DeWeaver 2007) between their 20th century simulations (20C3M) of sea ice extent and the observed record of ice extent during 1953–1995. The 10 selected GCMs simulated mean northern hemisphere ice extent during 1953–1995 within 20% of the observed mean in the Hadley Center sea ice and surface temperature data set (Had1SST; Rayner et al. 2003). This selection method emulated that used by Stroeve et al. (2007), except we used a 50% ice concentration threshold to define ice extent (as opposed to 15%). We chose a 50% cutoff because other studies have shown that polar bears select median to high sea ice concentrations (Arthur et al. 1996, Ferguson et al. 2000, Durner et al. 2006).

The satellite PMW data used in building the RSFs had 25 km × 25 km pixel resolution. However, sea ice grids among the 10 GCMs we analyzed had various model-specific spatial resolutions ranging from $\approx 1 \times 1$ to 3×4 degrees of latitude × longitude. To facilitate consistency among the RSF ice covariates, both with respect to the PMW covariates used to derive the RSFs and to the various GCM resolutions, we resampled the GCM grids to match the PMW grid. Each GCM native grid of sea ice concentration was converted to an Arc/Info (ver. 9.2; ESRI, Redlands, Ca, USA) point coverage and projected to the PMW polar stereographic coordinate system. A triangular irregular network (TIN, Arc/Info) was created from the point coverage using ice concentration as the z-value, and a 25 km pixel resolution grid was generated by sampling the TIN surface.

Effectively, this procedure over-sampled the original GCM resolution using linear interpolation.

Covariates of the resource selection functions

To build and extrapolate the RSF models, we required an identical suite of covariates (predictor variables) from both the observational sea ice data and the GCM sea ice projections. Both data sources contained an estimate of total sea ice concentration for each 25 km × 25 km pixel, which we termed *totcon*. Because prior RSF habitat analyses of polar bear locations and PMW data (Durner et al. 2004, 2006) showed non-linear associations between bear distributions and *totcon*, we also included a 2nd order effect (*totcon^2*). We further defined 3 covariates based on ice concentration thresholds. Thresholds were established as pixels containing ≥15% ice, pixels containing ≥ 50% ice, and pixels ≥ 75% ice. From each pixel in the study area, we measured the distances to the nearest pixel that met each of the 3 concentration thresholds. Hence, in addition to *totcon* and *totcon^2*, each pixel in the study area included the covariates of distance to ≥ 15% ice (*dist15*), distance to ≥ 50% ice (*dist50*), and distance to ≥ 75% ice (*dist75*). The spatial distributions of ice concentration thresholds varied among seasons, but were generally concordant with coastlines during winter in most of our study area (because ice concentration exceeded 75% throughout).

We included a fifth covariate defined as the distance between each pixel in the study area to the nearest coastline (*dist2land*). Last, we assigned ocean depth (*bath*) as a covariate to each pixel in the study area based on the IBCAO bathymetry chart. Therefore, each pixel, in both the data used to build the RSFs and in the data used to extrapolate the RSFs, included a total of 7 habitat covariates: *totcon*, *totcon^2*, *dist15*, *dist50*, *dist75*, *dist2land* and *bath*.

Defining seasons

We created 4 seasonal RSF models from the 1985–1995 observational record of PMW sea ice distributions and polar bear tracking data. Instead of defining seasons based on fixed boundaries between calendar months, we defined 4 temporally dynamic seasons (maximum, melt, minimum, and growth) based on the timing and amplitude of the intrinsic annual oscillation of ice growth and melt. Our intent for classifying months into dynamic seasons was designed to accommodate future changes in the timing and duration of ice growth and melt when applied to the 21st century GCM ice projections.

Our seasonal classification of any given month was determined by a threshold of sea ice change relative to the year-specific amplitude in sea ice extent (Fig. 2a). First, a month was assigned to the ice maximum season if that month's total ice extent in the study area (excluding East Greenland) was greater than the year-specific maximum ice extent minus 15% of the total change in annual extent (e.g., the amplitude of the annual ice extent oscillation). East Greenland was excluded because seasonal (melt/freeze) sea ice extent south of Fram Strait is confounded by large amounts of wind-driven ice export (Kwok et al. 2004). An inverse of this algorithm was applied to classify months into the ice minimum season. Finally, the remaining unclassified months (during the intervening periods) were assigned to either the ice-melt or ice-growth season depending on their chronology relative to the maximum and minimum seasons. The resulting seasonal designations throughout both the PMW and GCM periods, therefore, varied among years (Fig. 2b). Henceforth, we refer to the ice maximum, melt, minimum, and growth seasons as winter, spring, summer, and autumn, respectively.

Defining habitat available to polar bears

Our procedures for estimating the RSF models were based on used habitat versus available habitat, following the methods for discrete-choice modeling (Arthur et al. 1996, McCracken et al. 1998, Cooper and Millspaugh 1999, Durner et al. 2004, Durner et al. 2006, Johnson et al. 2006). For each polar bear location we defined the habitat that was available to that bear as the area within a circle, the center of which was the bear's previous location (Fig. 3; Arthur et al. 1996, Durner et al. 2004). The radius of the circle was determined by the elapsed time between the 2 consecutive observations, and by the distance a polar bear could travel during that time. Because movement rates of female polar bears vary by month (Amstrup et al. 2000), we calculated an expected movement rate (upper bound) for each month, and a unique radius for each pair of bear locations using the following equation:

radius of available habitat =
$$\{a + (b \times 2)\} \times c;$$

where a equals the mean hourly movement rate for all bears within the respective month; b is the standard deviation of the movement rate; $\{a + (b \times 2)\}$ gives an approximation of the upper limit to the hourly movement rate; and c equals the number of hours between locations. On rare occasions, the actual straight-line distance traveled by a bear between observations exceeded the calculated radius. In these cases, the radius of available habitat was defined as the straight-line distance actually traveled.

All pixels enclosed by the resulting availability circle were used in the RSF analysis (Fig. 4). Every enclosed pixel was considered a potential habitat choice (coded AVAILABLE) that the bear could have made as it traveled from its starting location, except the pixel containing the end location which represented the bear's selection (coded USED). Because the radius for each pair of locations was dependent on the elapsed time multiplied by a month-

specific movement rate, the number of available pixels varied among location pairs. In summary, each choice set (AVAILABLE and USED pixels) represented a census of discrete habitat units available to a bear for the respective starting point of a location pair. Each pixel within every choice set included all 6 habitat covariates.

Estimating the resource selection functions

We screened the 6 habitat covariates (main effects) for within-season correlations before developing a set of 30 *a priori* RSF models (Table 2). Pairs of main effects that were correlated ($|r| \geq 0.6$; Pearson's Correlation Coefficient; Conover 1980) within a season were not allowed in the same model. Durner et al. (2006) identified total ice concentration (*totcon*) as a critical habitat characteristic because polar bears are rarely found in open water, and a value *totcon* > 0 indicates sea ice is likely present. Thus, *totcon* was always entered as the initial covariate in all models.

We used a discrete-choice model to estimate model coefficients and Akaike's Information Criterion (AIC; Burnham and Anderson 2002) to rank models within each season. All pairs of starting and ending locations within each season entered each seasonal model. The discrete choice model was estimated by maximizing the multinomial logit likelihood (Manly et al. 2002). This was accomplished using the stratified Cox proportional hazards likelihood maximization routine available in the SAS procedure PROC PHREG (SAS Institute 2000). Although PROC PHREG was not designed to fit discrete choice habitat selection functions, Kuhfeld (2000) describes a method by which PROC PHREG can be adapted to maximize the appropriate discrete choice likelihood function. Standard errors of coefficients in each season were estimated by resampling, with replacement, a random subset (bootstrapping) of individual bears 2,000 times.

Following the estimation of parameter values and AIC, models were ranked according to Akaike weights (Burnham and Anderson 2002) from "best" (highest Akaike weight) to "worst." Akaike weights provided a standardized AIC ranking among the suite of candidate models where the sum of model weights is 1. Relatively large increases in Akaike weights indicated large improvements between competing models. AIC rankings and weights were compared to those obtained using the Bayesian Information Criterion (BIC; Burnham and Anderson 2002), which applies higher penalties for models fit to large data sets. BIC values were calculated as $-2log(L) + p[log(n)]$, where *log* was the natural logarithm (base *e*), *L* was the value of the multinomial logit likelihood evaluated at the maximum likelihood estimates, and n was the number of choice sets, or polar bear locations. Final RSF predictions of habitat selection involved model averaging within each season (Burnham and Anderson 2002), unless the AIC or BIC weights suggested there was only one reasonable model. Each *a priori* model within a season was used to predict every pixel's relative probability of selection (use by a polar bear), and a weighted average probability was computed across all models based on their AIC weights.

Assessing the resource selection functions

We applied an empirical method to assess performance of the models by comparing the RSF values of pixels selected by polar bears (used pixels) to the range of RSF values throughout the study area. Monthly RSF-value maps were constructed for the entire study area by applying the appropriate RSF seasonal model (depending on the respective month's seasonal classification as described above) to every ice-covered pixel throughout the study area based on each pixel's individual habitat covariates. Each monthly RSF-value map was projected to an equal area projection (Lambert

Azimuthal) and partitioned into 20 equal area zones along an increasing RSF-value gradient. In other words, each zone represented 5% of the available habitat across the study area (in the respective month); and the zones were labeled 1–20, with 20 representing the zone of highest relative RSF-value. Each polar bear location (n=19,901, 1985–2006) was intersected with its respective monthly map of equal area RSF zones, and associated with the zone-number occupied. Frequencies of polar bear occupancy within the 20 zones were evaluated against the null expectation that occupancy would be equivalent among the 20 zones if polar bears exhibited no selection preference among the 6 habitat covariates.

Extrapolating monthly RSF maps

Twelve monthly RSF-value maps were generated annually using the season-specific RSF model that corresponded with each month's seasonal classification. RSF values (the relative probability of polar bear utilization) were calculated for each 25 km × 25 km study-area pixel based on its respective habitat covariates. Monthly RSF maps were created for: 1) the observed PMW sea ice record (1979–2006); 2) the late 20th century ice simulations by 10 GCMs (~1950–2000); and 3) the 21st century ice projections by the same 10 GCMs (2000–2100). A total of 39,360 monthly RSF-value maps were created from the full suite of observed and modeled (Table 1) sea ice data sets.

Defining optimal polar bear habitat

The RSF represents the relative probability of use of a resource unit and it is proportional to the exponential linear function of the covariates. Magnitudes of RSF values are established by the unique combination of covariates and coefficients composing the specific models. Therefore, raw RSF values generated by a model for one season (e.g., spring) cannot be compared directly to or combined with those generated by a model for another season (e.g., winter). To assess annual changes in polar bear habitat over time we needed to develop a common metric that would allow the information in RSF values to be pooled, regardless of the model generating them. We did this by establishing a season-specific RSF threshold that distinguished "optimal" habitat (based on observational data) from non-optimal habitat.

Histograms of all polar bear location data gathered between 1985 and 1995 revealed that at least 70% of bear locations consistently occurred in the upper 20% of RSF-valued area. We defined optimal habitat, therefore, as the average RSF value that separated the upper 20% from the lower 80% of the RSF-valued area for each season. All mapped pixels with raw RSF values greater than the upper 20% threshold, therefore, were included in optimal habitat. In this way we converted RSF values, which cannot be pooled, to the number of square kilometers of mapped pixels of optimal habitat, which can be pooled.

We pooled the outputs of the 4 seasonal RSF models into an annual metric by extracting the monthly area (km^2) of optimal habitat, and summing the 12 monthly areas to arrive at a cumulative annual area of available optimal habitat. The cumulative annual area of optimal habitat was calculated within each IUCN unit (and combinations of units, Fig. 1) for all years of the observed satellite sea ice record, as well as the late 20th century hindcast simulations and 21st century ice projections by the 10 GCMs (Table 1).

We used the baseline period 1985–1995 to define high-value (optimal) habitat because during this early period of our studies, year-round polar bear movements were less restricted than during the more recent years of reduced sea ice extent. We expressed 21st century changes in the amount of optimal habitat as percent change relative to this 20th century baseline. We emphasize that our 4 seasonal thresholds,

derived from the 1985–1995 period, remained fixed. Thus, when we extracted the area of optimal habitat from the 21st century maps of RSF, the threshold values remained those that were observed in 1985–1995. This approach created a foundation that allowed us to examine whether future ice projections indicated increases, decreases, or stability in the cumulative annual area of optimal polar bear habitat – relative to our earliest decade of empirical observations. Inherently, this approach assumes that polar bears in the future will select habitats in the same way they did between 1985 and 1995 despite dramatic seasonal changes in ice extent and distribution.

Quantifying changes in polar bear habitat

Absolute and percent-change metrics of sea ice extent, RSF value, and optimal habitat area were used to quantify 20th and 21st century changes and trends in the study area. Changes were examined temporally for within individual IUCN units, grouped units, and for the study area as a whole (Fig. 1). We also assessed variability among GCMs in their predictions of sea ice cover and polar bear habitat. We used linear least squares regression to examine rates of change in the area of optimal habitat. Analyses were conducted for the 21st century as a whole and on selected decadal time periods.

Results

Polar bear location data

The 1985–1995 polar bear location data used to construct the RSF models were distributed throughout the study area (Fig. 5), however, sample sizes varied considerably between IUCN units (Table 3). Over 66% (Table 3) of the polar bear locations available for estimating RSFs were from the Chukchi Sea and Southern Beaufort Sea. Bear locations in the Laptev Sea

and the Arctic Basin made up an additional 25%. The total number of collared bears and bear locations used for estimating seasonal RSFs was greatest in winter and lowest in autumn (Table 4).

Contributions from the different jurisdictions varied. The greatest number of samples came from the United States and the smallest from the Denmark (Greenland; Table 5). A total of 12,171 used and 1,310,805 available habitat records were in the 1985–1995 period (Table 5). A similar jurisdictional distribution, albeit with smaller sample sizes, occurred in the 1996–2006 data (7730 used and 722,405 available records; Table 5).

Seasons

Defining seasons based on changes in ice extent rather than a calendar-date convention resulted in modest annual variation in their chronology and duration. Within the full observational period (1985–2006), winter began in November (2 years), December (7 years), or January (2 years), and continued to April (1 year) or May (10 years). Spring began in May (1 year) or June (10 years) and continued to July (9 years) or August (2 years). Summer was represented by August and September (9 years) or by September only (2 years). Autumn always began in October, often included November (9 years), and rarely included December (2 years).

Average length of seasons over the 21st century remained generally unchanged (Fig. 6). Overall, for both the observed and modeled ice data, duration of winter averaged ~6 months and other seasons averaged ~2 months each. There was a slight increase in mean length of the summer season during the latter half of the 21st century caused by a few GCMs that projected near ice-free summers, such as run-1 for CCSM3 (Fig. 2b), where the number of months comprising the summer season increased after about 2065. Longer summer seasons were typically compensated by shorter winter seasons.

Resource selection functions

Correlations between RSF covariates (Pearson's $|r| > 0.6$; Table 6) reduced the number of candidate RSF models. Twenty models were estimated for winter, 28 for spring, 30 for summer, and 24 for autumn (Table 2; Appendix A1–A4). The top models (Appendix A1–A4) for every season had AIC and BIC weights >0.99. Therefore, the pooled contribution from all models within a season was heavily weighted by the covariate estimates of the best model, so model averaging was effectively inconsequential and omitted. The top model for the winter season contained *totcon*, *totcon*^{2}, *bath* and *dist2land* (Table 6). The top models for the remaining seasons all contained *totcon*, *totcon*^{2}, *bath* and *dist15*.

Despite overall similarity among the 4 seasonal RSF model structures, differences in the magnitude of the parameter estimates indicated that there were seasonal differences in polar bear habitat selection (Fig. 7). Standardized plots of relative selection probability, assuming all other variables are held constant at their respective medians, showed that selection decreased with increasing values of *bath*, *dist2land*, and *dist15*. Owing to a *totcon* quadratic covariate in each model, the relative probability of selection increased as total ice concentration increased up to approximately 95%, 80%, 65%, and 60% for winter, spring, summer and autumn, respectively, and then declined with further increases in concentration.

Selection for shallow water was strongest in the winter, and weakest in the summer (Fig. 7). During winter, the standardized RSF value for 1,300 m depth was 0.6, but an equivalent RSF did not occur in summer until depths of 3,000 m. Polar bears showed the strongest selection for the 15% sea ice concentration threshold in autumn, reduced selection in summer, and lowest selection in spring (Fig. 7). During winter, distance to land was a stronger covariate than distance to the 15% sea ice concentration

threshold; but because these 2 covariates were highly correlated in winter ($r = 0.76$; Table 6), they may be considered partly equivalent.

Resource selection function assessment

Frequency distributions of observed polar bear locations within equal area RSF intervals resembled an exponential function, confirming the RSF models possessed the hypothesized ability to distinguish habitat selection among the 6 covariates (Fig. 8). During 1985–1995 and 1996–2006, 71.2% and 82.3% of polar bear locations, respectively, occurred in the upper 20% of the RSF-valued habitat area (the 4 highest-valued RSF equal area intervals). The upper 20% of RSF-valued habitat area encompassed a majority (> 70%) of polar bear locations, so (as described earlier) we used the lower bound of the 17th (of 20) 5% equal area interval to distinguish pixels of "optimal" polar bear habitat from all other RSF pixels.

Resource selection function maps

Individual monthly RSF maps represent the basic elements we used for assessing future habitat changes and trends, so it is beneficial to illustrate their content and highlight a few general patterns in RSF habitat distributions, seasonal trends, and variability among the GCMs (Fig. 9). First, it is apparent that higher-value RSF habitat occurs mainly around the peripheral shelf-waters of the polar basin and never in the deep-water central basin, largely owing to the negative effect of the bathymetry covariate (Fig. 7). Second, comparing a representative summer month (September 1985) from the early decade (1985–1995) to a recent month of record minimum ice extent (September 2005) exemplifies the losses of summer habitat that polar bears have already experienced, especially in the Alaska-Eurasia region (Fig. 9a). Third, there is considerable variability among the 10 GCMs in their

projections of summer habitat extent and distribution during the mid- and late-21st century (Fig. 9b); and fourth, habitat changes are far less pronounced and less variable among GCMs during winter (Fig. 9c).

21st century habitat trends

To understand trends in polar bear habitat, it is helpful to first consider the general trends predicted for sea ice. All 10 GCMs predict a downward trend in sea ice extent, with a more pronounced downward trend during summer (Fig. 10a). Even in the CCSM3 ice projections based on the SRES-B1 scenario (forcing scenario with less greenhouse gas loading), sea ice was projected to diminish, albeit less rapidly (CCSM3_041; Fig. 10a). Despite overall agreement in the direction of change, the 10 GCMs we considered varied in the estimated amount of total ice extent and rate of change. Disparities between the satellite-observed extent of ice and the GCM estimates, as well as the disparities between GCMs, reflect aspects of model uncertainties that are introduced by a myriad of factors (DeWeaver 2007). Compared to the observed ice extent, the GCM ensemble mean overestimates ice extent in the study area in both the late-20th century simulations and the early-21st century projections (Fig. 10a). Furthermore, the recent rate of summer ice decline in the observed data shows a trajectory that is steeper than that of the GCM ensemble mean during the early 21st century, reiterating Stroeve et al.'s (2007) conclusion that Arctic sea ice may be disappearing at a rate that is "faster than forecasted".

For purposes of this study, we are more interested in the amount of change that is projected by the GCMs, and less about accuracy of any one GCM's initial estimate. Therefore, we calculated each model's percent change relative to itself (Fig. 10a, right). Baselines for calculating percent change used the 1990–1999 mean for the observed ice record and the 20th century ice simulations, and the 2001–2010

mean for the 21st century projections. The ensemble mean indicated an approximate 75% loss in summer ice extent by the end of century, with the greatest rate of loss during mid-century. The notion of "faster than forecasted" remains clearly evident for the changes in summer ice extent. In contrast, the projected percent change in winter ice extent is notably smaller and much more consistent among the GCMs.

A strong association between ice extent and RSF habitat value is apparent (Fig. 10b). Overall, reduced ice cover infers less value in available polar bear habitat because the spatial pattern of ice melt is generally from the periphery poleward (i.e., coastal and shelf water habitats are melting first). All GCMs overestimated summer RSF habitat value compared to observations, and most GCMs overestimated the observed habitat value in winter. The GCM ensemble mean shows that about 60% of the summer RSF habitat value is lost by the year 2100. The CCSM3 B1 forcing scenario projected RSF habitat value to decline to approximately 45% of pre-2000 levels (Fig. 10b). Relatively little change is predicted for winter RSF habitat value.

Projected rates of change in cumulative annual area of optimal polar bear habitat during the 21st century varied considerably among the IUCN units and groups (Fig. 11). Within the Alaska-Eurasia group (Fig. 11a), rates of decline are projected to be greatest in the Southern Beaufort, Chukchi, and Barents Sea IUCN units. Observed losses in these 3 units compared to the Laptev and Kara Sea units suggests that 'faster than forecasted' trajectories may be more (or less) pronounced at regional scales. In comparison, optimal habitat changes in the Queen Elizabeth and Arctic Basin units of the Canada-Greenland group (Fig. 11b) are projected to be negligible if not increasing; but note that very little optimal habitat existed in the Arctic Basin to begin with (12 month sum of 18×10^3 km^2 compared to 985×10^3 km in the southern Beaufort Sea), so the positive percent-

change represents only a small increase in habitat area. The CCSM3 predictions by the B1 forcing scenario were often similar to the ensemble mean until approximately 2030 (Fig. 11a and 11b).

Net annual habitat changes were comprised of dramatic summertime losses ameliorated by relatively little change during the long winter season (Fig. 12). In the full study area (Fig. 12a), optimal habitat was always most abundant in winter, and winter losses over the 21st century were relatively modest. In contrast, optimal habitat was less extensive during spring and summer, and projected to diminish by as much as 55–70% by 2100. Because little change is predicted for half of the year (winter), average annual habitat losses in the range of 30% (Fig. 12a) translate to spring and summer losses that are about two times greater.

Large declines in optimal habitat are projected to occur in the Alaska-Eurasia region where 60–80% of the polar bears' historical area of spring and summer habitat may disappear by the end of the century (Fig. 12b). The Canada-Greenland region (Fig. 12c) has historically contained less total optimal habitat area, primarily because it is a smaller geographic area than the Alaska-Eurasia region. Nevertheless, while there is a similar seasonal pattern to the projected losses of optimal habitat, the magnitude is much less owing to the predicted stability of ice in the Queen Elizabeth region (Fig. 11b).

The projected rates of habitat loss over the 21st century are not constant over time (i.e., non-linear; Figs. 12a-c). Rates of loss tend to be greatest during the second and third quarters of the century and then diminish during the last quarter (Figs. 10 and 11). Losses in optimal habitat from 1985–1995 to 1996–2006 establish an observed trajectory of change that is remarkably consistent with the GCM projections, however, if the observed rate of change (established over a 1 decade period) is extrapolated over the first half of the 21st century, more habitat is lost than that projected by the GCM ensemble average (i.e., faster than forecasted; Fig. 12).

Rates of change in the cumulative area of optimal sea ice habitat were statistically significant ($\alpha = 0.01$) in the 21st century for most IUCN units, the two grouped IUCN regions, and the study area as a whole (Table 8). The sole exception to this was the Arctic Basin, which saw a statistically significant ($\alpha = 0.05$) 1.6% / decade increase in the amount of optimal habitat available in the 21st century. However, the Arctic Basin represented a very small portion (2,000 km^2) of the total observed (1979–2006) amount of annual optimal habitat in the study area. The average rate of change for the entire study area was estimated to be -4 % / decade. Decreases of optimal habitat ranged from -0.9 (Queen Elizabeth) to -6.5 (Barents Sea) % / decade. Notably, 4 of the 10 GCMs (CCSM3, HadGEM, MIROC, and MPI) projected near depletion of all optimal habitat (year-round) in the Barents Sea IUCN.

Spatial changes in optimal polar bear habitat

Optimal polar bear habitat in the polar basin declined between the early and latter decades of the observational record, from 1985–1995 to 1996–2006. The change varied spatially, however, across the study area (Fig. 13). Large declines in optimal habitat occurred in the Southern Beaufort, Chukchi, Barents, and East Greenland Sea IUCN units, while offsetting patches of habitat gain and loss resulted in little net change in the Laptev, Kara, Northern Beaufort, and Queen Elizabeth units. There was little optimal habitat in the Arctic Basin IUCN unit to begin with during 1985–1995 (< 13,000 km^2 when summed over 12 months), so the small increase of ~11,000 km^2 translated to a large percentage (~83%) increase. In comparison, the Southern Beaufort Sea unit experienced a net loss of ~64,000 km^2 of optimal habitat between 1985–1995 and 1996–2006, which translated to a -6.2% change.

13

The observed trends show decadal declines in optimal habitat that have been pronounced in the Alaska, eastern Siberia, Svalbard, and southern Greenland regions, and interspersed with gains (so little net change) over the shelf waters of the Laptev and Kara Sea, and the high-latitude interior Arctic along the Canadian Archipelago and northern Greenland (Fig. 13). The regions of most pronounced polar bear habitat loss in the past decade have occurred around the two geographic areas (Barents/Greenland Seas and the Chukchi Sea) where the Arctic Ocean incurs the largest exchanges of ocean water and ice export.

There was a remarkable degree of continuity between the projected changes in polar bear habitat throughout the 21st century (Fig. 14) and the changes that have already been observed at the century's onset (Fig. 13). The 21st century predictions perpetuate the already observed indications that the greatest proportional losses of optimal habitat are occurring in the Chukchi, Southern Beaufort, Barents, and East Greenland seas. The 21st century predictions indicate dramatic losses of optimal polar bear habitats around all coastal regions except the Queen Elizabeth region of the high-latitude Canadian Arctic (Fig. 14), where optimal habitat area is projected to be largely sustained (Fig. 11).

Discussion

Resource selection functions

We have established that habitat selection by polar bears can be modeled by coarse-scale landscape features in their environment. All 4 seasonal RSFs consisted of the same, or functionally similar, covariates. The response of polar bears to those covariates, regardless of season, was consistent in sign (direction) of the parameter estimates. Magnitudes of the covariate parameter estimates, however, did vary among the seasonal models, suggesting that while the same habitat covariates are

important throughout the annual cycle, their effects were seasonally dependent.

Previous studies of polar bear habitat relationships have identified the extent and composition of sea ice (or the lack thereof) as the ultimate driver of polar bear spatial patterns (Stirling et al. 1993, Arthur et al. 1996, Ferguson et al. 1997, Ferguson et al. 2000, Mauritzen et al. 2001, Durner et al. 2004, Durner et al. 2006). The polar bears analyzed for this study almost exclusively occupied pelagic regions. During the summer, when sea ice extent was at its annual minimum, most polar bears within the study area remained on the ice rather than retreating to land. It was reasonable, therefore, to include sea ice concentration in all of the *a priori* models for each season.

The RSF models were constructed to collectively quantify habitat selection by all polar bear populations throughout the polar basin. The distribution of the RSF emulated the basin-wide distribution of polar bears in the study area – more than 70% of polar bear locations occurred within the highest 20% of RSF-valued habitat (Fig. 8). There was consistency between the two observational periods, pre-1996 and post-1995, even though the later period included some of the most extreme melt seasons since 1979. Pooling the polar bear tracking data from throughout the Arctic obviously strengthened robustness of the models for basin-wide application. At regional scales, however, numerous factors would cause performance of the models to vary: 1) seasons are not synchronous between regions (Belchansky et al. 2004); and 2) a single suite of RSF covariates cannot entirely accommodate differences in habitat selection caused by regional differences in sea ice composition and dynamics (Wadhams 2000); and 3) the tracking data were disproportionately distributed (Fig. 5).

We observed differences in RSF performance among IUCN units (Table 9). Model performances tended to be less robust

over IUCN units spanning the broad Eurasian continental shelf, and more robust in the Barents Sea and the units bordering North America. Nevertheless, in all cases, the top 50% of the RSF-valued habitats were occupied by a substantive majority (>85%) of the polar bear locations demonstrating that the RSF models were robust at a variety of scales throughout the basin

Applicability of retrospective RSFs to 21st century sea ice predictions

Similarities among the four seasonal RSF models and their consistent ability to predict habitat selection during 1996–2006 (when sea ice conditions were substantially different) indicate that the RSFs possess robustness to substantial environmental changes. Furthermore, the four seasonal RSFs were developed independently, yet structures of the best models were very similar, indicating that the selected covariates are important to polar bears throughout the year.

Attaining a consistent set of model components, despite significant intra-annual variation in sea ice extent and distribution, suggests that those same model components will be important throughout future inter-annual sea ice changes. The strong performance of our models when applied to passive microwave (PMW) observations of sea ice offers further evidence of their validity with regard to future projections. More than 80% of the locations of polar bears observed between 1996 and 2006 were found in the top 20% of RSF-valued pixels (Fig. 8), as estimated by models that were constructed with data collected during a different time period (1985–1995).

This strong performance was despite the fact that 35.4% of the bear locations used to build the RSFs were collected inside the Chukchi Sea IUCN. The 1996–2006 data used to test RSF performance, however, were composed of only 2.9% Chukchi Sea data (Table 3). This high performance also occurred despite large

changes in sea ice during the post-1995 decade. Those changes included several of the greatest sea ice retreats of the observational record. These results support the validity of using RSF models built with retrospective data to predicting polar bear habitat in the 21st century from GCM sea ice projections.

Variability among GCMs

One source of uncertainty among GCM outputs rests in the greenhouse gas scenario used to force the models. The IPCC SRES forcing scenarios were designed to capture a range of political and societal responses to the economic and environmental concerns of global warming. Three SRES forcing scenarios, the B1, A1B, and A2, respectively attain CO_2 concentrations levels of 546, 717, and 856 ppm by the year 2100. Zhang and Walsh (2006) used these scenarios to calculate the decrease in ensemble-mean summer ice minimum area for 1979–1999 and 2080–2100 and obtained reductions of 45.8%, 59.7% and 65.0% of sea ice in for the B1, A1B and A2 scenarios, respectively.

Pragmatic reasoning led us to focus our analyses on the A1B "business as usual" scenario and exclude the A2 scenario. As would be expected, cursory comparisons with CCSM3 ice projections based on the SRES-B1 scenario (reduced carbon forcing; Figs. 10–11 and Table 7) showed that sea ice was projected to diminish less rapidly (Fig. 10a) and hence the loss of optimal polar bear habitat was less rapid (Fig. 11, Table 7). We anticipate the converse would be true for a forcing scenario that amplifies greenhouse gas loading (e.g. SRES-A2). But even the relatively optimistic B1 scenario, when applied by CCSM3, predicted as much as a 70% loss of optimal habitat in the Barents Sea (Fig. 11).

Close inspection of the CCSM3 ice projections shows that trajectories of the A1B and B1 forcing scenarios are almost uniform until about 2030, after which they begin an

obvious departure (Fig. 10a). Differences between the A1B and B1 scenarios (for the CCSM3 model) in timing and relative magnitude of projected sea ice extent are remarkably similar to the inverse of their imposed CO_2 loadings (see *http://www.cccma.ec.gc.ca/data/cgcm3/cgcm3_forcing.shtml*) as well as the resultant multi-model global average surface warming (Solomon et al. 2007; Fig. SPM.5).

21st century habitat distribution and trends

Predicted losses of polar bear habitat during the 21st century varied among GCMs and forcing scenarios. In general, declines in optimal sea ice habitat were accelerated from early in the 21st century until about 2075. Rates of habitat loss declined after 2075 because several models had already reached near ice-free summers by this time (Fig. 10).

The observed habitat changes from 1985–1995 to 1996–2006 established a trajectory that was generally perpetuated by the 21st century sea ice projections. In many cases, the observed rates of habitat change exceeded those of the GCMs, revealing a "faster than forecast" signature (Stroeve et al. 2007) in polar bear habitat loss as well as sea ice loss.

Rates and trends in observed habitat changes between 1985–1995 and 1996–2006 were not ubiquitous throughout the Arctic. The observational record revealed that the greatest losses of optimal polar bear habitat have occurred in the peripheral seas of the Arctic while interior regions (i.e., the Arctic Basin and Queen Elizabeth) were more stable (Fig. 13). In particular, the observational data showed the largest decline of optimal habitat in the Chukchi and Barents Seas, while only modest declines occurred in the Kara and Laptev seas. Disparities among peripheral IUCN units likely stem from oceanographic differences: both the Chukchi and Barents Sea are more directly influenced by the warmer waters of Pacific and

Atlantic Ocean, respectively (Macdonald and Bewer 1996, Woodgate et al. 2006). The magnitude of predicted habitat loss in most peripheral regions of the Arctic was not offset by modest increases in the interior polar basin; hence there was a net loss in optimal polar bear habitat during the observational period, 1985–2006.

Similar spatial patterns of habitat loss to that of the observational record are predicted for the mid-21st century (Fig. 14). Large habitat losses are also predicted, however, in the Kara and Laptev Seas, rendering those IUCN units consistent with the observed and projected declines in other Alaska-Eurasia IUCN units. In the Northern Beaufort Sea unit, little net change in optimal habitat was predicted until mid-century (Fig. 11b), after which net losses commenced in all but the most northerly sector (Fig. 14). Also similar to the observational period, the GCM projections continued to sustain optimal habitat in the Arctic Basin and Queen Elizabeth units until about 2050, and changes thereafter remain notably small.

By the end of the 21st century, the annual average area of optimal polar bear habitat declined to 1.0 million km^2 from its observed value of 1.5 million km^2 in 1985–1995 (-32% change, Fig. 12). This net change reflects the influence of ~6 winter months (Fig. 6) in which there was little change in optimal habitat combined with more dramatic changes during the spring, summer, and autumn (Fig. 12). In both the observational period and in the 21st century projections, the greatest reductions in optimal habitat occur during summer. By the mid-21st century, most peripheral seas have very little remaining optimal polar bear habitat during summer. Not only is there a spatial loss, but the length of summer is projected to increase slightly by the end of the 21st century.

In contrast, optimal polar bear habitat returns in winter throughout most of its former range. An exception to this, however, is the Barents Sea, where high-value RSF pixels were largely absent even during winter in the later part of the

21st century (Fig. 9). Collectively, spring and summer represent ~4 months of the annual cycle (Fig. 6), so the loss of optimal habitat during spring and summer has temporal, as well as spatial, significance.

While trends in habitat change were similar to changes in sea ice, sea ice alone did not fully explain the distribution of polar bear habitat because ocean depth was a strong covariate in all seasons. Persistent sea ice in the Arctic Basin IUCN units did not translate into large areas of optimal habitat because the region is predominantly deep water. The nearby Queen Elizabeth unit, however, which had ice characteristics similar to the Arctic Basin, but also encompassed shallow continental shelf waters, experienced an increase of high-value RSF habitat by the mid-21st century (Fig. 14).

Ecological interpretation of the RSF covariates

Polar bears in the pelagic ecoregion selected ice concentrations near 80% in spring, 65% during summer, 60% in autumn, and 95% in winter. In the Canadian archipelago Ferguson et al. (2000) found that polar bears were highly selective for habitats with > 90% sea ice throughout the year. Ferguson et al. (2000) also observed that even within the seasonal ice ecoregion of Baffin Bay, polar bears selected sea ice concentrations ≥ 95% during autumn through spring. Only during summer in Baffin Bay (seasonal ice ecoregion) did polar bears demonstrate selection for ice concentrations <70% (Ferguson et al. 2000). Durner et al. (2004) found that polar bears in the Beaufort Sea selected sea ice near 100% concentration in spring and 70-80% in autumn. The selection for moderate sea ice concentration that we observed during spring through autumn throughout the pelagic ecoregion was similar to that reported by Mauritzen et al. (2003a) in the Barents Sea, and by Arthur et al. (1996) and Durner et al. (2006) in the Chukchi Sea. The results of these studies suggests that spatial patterns of polar

bears vary among the ecoregions defined by Amstrup et al. (2007) and that it is appropriate to define ecoregion-specific habitat models.

The seasonal variation in selection of ice concentration may imply a functional response (Mauritzen et al. 2003a) by polar bears to balance foraging and refuge requirements; bears position themselves in the most optimal habitat for hunting seals but at the same time select sea ice that will provide safety from ocean storms or becoming separated from the main ice pack. This may explain why polar bears used areas with relatively high ice concentration in close proximity to areas with very low (15%) ice concentrations during spring through autumn. In a study of polar bear spatial patterns in the Barents Sea, Mauritzen et al. (2003a) observed similar behavior by bears to avoid low ice concentrations near the open ocean.

Similar to total sea ice concentration, response to the 15% ice concentration threshold varied seasonally. As the spring melt begins, polar bears continued to use areas with relatively high ice concentrations, but they also showed the lowest degree of selection for the 15% ice threshold, possibly to avoid the open ocean near the edge of the retreating pack. The opposite occurred during autumn, which, as a season of ice extent similar to spring, polar bears showed greater selection for the 15% ice threshold than at any other time of year. Different response to the 15% threshold in spring and autumn suggests an ability of bears to anticipate seasonal changes in sea ice (Ferguson et al. 2000). It is likely that polar bears in the pelagic ecoregion position themselves near the autumn ice edge to expedite their return to hunting habitats over shallow continental shelf waters.

Distance to land, rather than distance to the 15% ice concentration threshold, entered the best winter RSF, but these two covariates were highly correlated in winter and can be considered functionally equivalent. Although polar bears selected high ice concentrations during winter, selection for sea ice near shore

may be an attempt by polar bears to maintain close proximity to the broken sea ice in near shore flaw zones and polynyas where prey may be most available (Stirling et al. 1993, Stirling 1997).

Polar bears throughout the pelagic ecoregion selected ice over relatively shallow seas throughout the year. The response that we observed was similar to that of Durner et al. (2004) who reported that polar bears in the Beaufort Sea selected habitats over the shallowest waters available. Polar bear distribution relative to ocean depth appears consistent with expected prey distribution. Polar bears within the study area are mostly dependent on young of the year ringed seals (Stirling and Ortsland 1995), whose distribution is primarily in broken ice over shallow waters (Born et al. 2004). Polar bears also prey on bearded seals, whose benthic feeding habitats (Burns 1981) generally limit their distribution to open ice habitats over the continental shelves (Gjertz et al. 2000). Therefore, the response of polar bears to bathymetry, as it appears in the RSFs, is consistent with expected prey distributions.

Consequences of habitat change on polar bear distributions

There were large spatial differences during summer between the observed and projected amounts and distributions of optimal polar bear sea ice habitat. This evokes questions regarding the movements and distribution of polar bears as they contend with what may be extreme minimum ice seasons in the future. We suggest that polar bears living in the polar basin will be required to "make decisions" in response to increasing seasonal amplitudes in sea ice extent. They must either follow the sea ice to higher latitudes where the ice may persist (but possibly over less productive waters), or choose to remain nearby their traditional foraging ranges by summering on land and fasting. Bears that move north in the summer with the retreating

sea ice then must decide if returning to traditional nearshore winter areas is a better option than simply remaining in an area where sea ice is relatively persistent throughout the year.

Alaska-Eurasia polar bears which follow the retreating pack ice over the summer will enter regions already occupied by other populations of polar bears (i.e., Queen Elizabeth, Northern Beaufort, and Arctic Basin). The carrying capacity of polar bear habitat is unknown, but the relatively small world population is distributed over a large geographic region. This suggests that, as the world population of polar bears is forced into smaller areas of optimal habitat, individual reproductive fitness will likely decline because of density dependent effects (McLoughlin et al. 2006).

Polar bears have fidelity to geographic regions (Amstrup et al. 2000) such that populations may be defined by the movements of individuals (Taylor et al. 2001, Mauritzen et al. 2002, Amstup et al. 2004). It is reasonable to assume that individuals would attempt to return to their region of origin even when their habitat undergoes extreme seasonal redistribution. This may be accomplished by either summering on land adjacent to traditional regions, or following the ice north to remnant summer ice refugia and returning to traditional ranges when the ice grows in autumn.

Either following the ice or summering on land likely imposes different energetic costs (Mauritzen et al. 2003b). Available evidence suggests that polar bears are largely food deprived while on land (Ramsay and Hobson 1991). Therefore, polar bears that summer on land must gain sufficient weight prior to going ashore to survive an extended fast. While summering on land has been an effective strategy for some populations of polar bears living in prey-rich environments, such as Hudson Bay, recent evidence suggests there are limitations, even in those regions, to the amount of time that polar bears can remain on land and still maintain a viable population (Stirling and

Parkinson 2006, Regehr et al. 2007). Polar bears in the Beaufort Sea do not reach their peak body condition until late autumn or early winter (Durner and Amstrup 1995), suggesting that an extended summer fast may not be possible for some populations in the polar basin. In contrast, while pack ice over deep water likely has lower prey densities than ice over the continental shelves, some prey may be available to polar bears that choose to spend the summer on the pack ice (Mauritzen et al. 2001).

Assuming that the RSF predictions of polar bear habitat are robust, by the mid-21st century most bears choosing to follow the retreating spring sea ice will occupy coastal zones in the Queen Elizabeth area and the most northern reaches of the Northern Beaufort IUCN unit during summer. Distances traveled between summer and winter ranges will be greatest for those bears that winter along the Eurasia coast and least for bears that winter near the Canadian coast. Polar bears are capable of sustained movement rates > 4 km / hr (Amstrup et al. 2000) and may travel an average of > 5,000 km / year in response to seasonal extremes in sea ice distribution (Garner et al. 1990).

Extensive movements to and from remnant summer habitats and traditional winter ranges, however, will likely impose greater energetic demands on some age/sex classes compared to others (Derocher and Taylor 1994). Polar bears have demonstrated fidelity to geographic regions for maternal denning (Ramsay and Stirling 1990, Amstrup and Gardner 1994). For pregnant polar bears, returning to traditional denning locales could become energetically prohibitive if they chose to summer on high-latitude ice cover. Pregnant polar bears must have adequate lipid reserves prior to denning to maximize survival of their neonates (Atkinson and Ramsay 1995). Lactation imposes additional energy demands on females with young (Thiemann et al. 2005). Mobility of females with first year young is less than that of other reproductive classes (Ferguson et al. 1997, Amstrup et al. 2000) and they may avoid active

drift ice (Mauritzen et al. 2003b). Therefore, long distance movements to and from the Alaska-Eurasia region may place the greatest demands on pregnant bears and bears with dependent young, and may ultimately impact reproductive fitness and population recruitment.

Conclusions

We developed RSF models of polar bear habitat utilization using empirical data of polar bear movements and sea ice conditions during 1985–1995 in the Arctic Ocean and peripheral seas of the polar basin. We then extrapolated the RSF models using 1) observed sea ice conditions during 1996–2006, and 2) projected sea ice conditions during the 21st century, to assess both recent and future changes in the extent and distribution of polar bear habitats in the polar basin. The 21st century sea ice projections were extracted from 10 IPCC AR-4 general circulation models which had 20th century ice simulations that were reasonably concordant with the observational sea ice record of minimum summer ice extent. The following points summarize the main results of this study:

- Polar bears prefer habitats that are over shallower water (continental shelf), partially covered by sea ice, and closer to land during winter. Loss of sea ice typically translates to loss of preferred polar bear habitat because the spatial pattern of melt is generally from the periphery of the ice pack (shelf waters) poleward.

- Declining ice trends are pronounced in summer but the ice cover is largely restored each winter, so amplitude of the annual oscillation in sea ice extent increases. Hence, changes in polar bear habitat extent take on strong seasonal dependency, with dramatic losses in summer and modest to negligible losses in winter.

- Observed decadal changes from 1985–1995 to 1996–2006 show pronounced losses of polar bear habitat during the spring and summer in the southern Beaufort, Chukchi, Barents, and East Greenland seas. Projected habitat losses during the 21st century are spatially and seasonally consistent with the trajectories already established by the past 2 decades of observational data, with the addition of pronounced losses in the nearshore regions of Laptev and Kara seas.

- By the end of the 21st century, only modest net annual habitat losses are predicted for areas north of the high-latitude Canadian archipelago and Greenland, affording these regions of the polar basin the greatest likelihood of sustaining viable polar bear populations.

- Increased seasonal swings in ice extent will require polar bears inhabiting Alaska and Eurasia to either migrate long distances to remain on the ice or spend summers stranded on land. Either scenario presents energetic challenges that could jeopardize long-term residency of the Alaska-Eurasia polar bear sub-populations.

- Observed rates of habitat loss during the past 2 decades define a trajectory that is greater than most GCMs predict (e.g., faster than forecast), so projected habitat losses based on multi-model averages may be conservative.

Acknowledgements

References Cited

Aars, J., N.J. Lunn, and A.E. Derocher. (Editors). 2006. Polar Bears: Proceedings of the 14th Working Meeting of the IUCN/SSC Polar Bear Specialist Group, 20–24 June 2005, Seattle, Washington, Occasional Paper 32.

Amstrup, S.C. 2003. Polar bear, *Ursus maritimus*. Pages 587-610 in G.A. Feldhamer, B.C. Thompson, and J.A. Chapman (Editors). Wild Mammals of North America: Biology, Management, and Conservation. Johns Hopkins University Press, Baltimore, Maryland, 2nd edition.

_____, G.M. Durner, I. Stirling, N. Lunn, and F. Messier. 2000. Movements and distribution of polar bears in the Beaufort Sea. Canadian Journal of Zoology 78:948-966.

_____, and C. Gardner. 1994. Polar bear maternity denning in the Beaufort Sea. Journal of Wildlife Management 58:1-10.

_____, B.G. Marcot, and D.C. Douglas. 2007. Forecasting the Rangewide Status of Polar Bears at Selected Times in the 21st Century. USGS Alaska Science Center, Anchorage, Administrative Report.

_____, T.L. McDonald, and G.M. Durner. 2004. Using satellite radiotelemetry data to delineate and manage wildlife populations. Wildlife Society Bulletin 32:661–679.

_____, I. Stirling, T.S. Smith, C. Perham, and G.W. Thiemann. 2006. Intraspecific predation and cannibalism among polar bears in the Southern Beaufort Sea. Polar Biology 29: 997–1002.

Arthur, S.M., B.F.J. Manly, L.L. McDonald, and G.W. Garner. 1996. Assessing habitat selection when availability changes. Ecology 77:215–227.

Atkinson, S.N., and M.A. Ramsay. 1995. Effects of prolonged fasting of the body composition and reproductive success of female polar bears (*Ursus maritimus*). Functional Ecology 9:559-567.

Belchansky, G.I., D.C. Douglas, and N.G. Platonov. 2004. Duration of the Arctic sea ice melt season: Regional and interannual variability, 1979–2001. Journal of Climate 17:67–80.

_____, _____, and _____. 2005. Spatial and temporal variations in the age structure of Arctic sea ice. Geophysical Research Letters 32:L18504.

Bodmer, R.E., J.F. Eisenburg, and K.H. Redford. 1997. Hunting and the likelihood of extinction of Amazonian mammals. Conservation Biology 11:460–466.

Born, E.W., J. Teilmann, M. Acquarone, and F.F. Riget. 2004. Habitat use of ringed seals (*Phoca hispida*) in the North Water area (North Baffin Bay). Arctic 57:129–142.

Burnham, K.P., and D.R. Anderson. 2002. Model Selection and Multimodel Inference. Springer-Verlag, New York, 2nd edition.

Burns, J.J. 1981. Bearded seal *Erignathus barbatus* Erxleben, 1777. Pages 145–170 in S.H. Ridgeway and R.J. Harrison (Editors). Handbook of Marine Mammals. II: Seals. Academic Press, London, United Kingdom.

Cavalieri, D., P. Gloerson, and J. Zwally. 1990. DMSP SSM/I daily polar gridded sea ice concentrations, June to September 2004. In J. Maslanik and J. Stroeve (Editors). National Snow and Ice Data Center, Boulder, Colorado, Digital media.

Comiso, J.C. 2006. Abrupt decline in the Arctic winter sea ice cover. Geophysical Research Letters 33:L18504.

Conover, W.J. 1980. Practical Nonparametric Statistics. John Wiley and Sons, New York, 2nd edition.

Cooper, A.B., and J.J. Millspaugh. 1999. Application of discrete choice models to wildlife resource selection studies. Ecology 80:566–575.

Davies, K.F., C.R. Margules, and J.F. Lawrence. 2004. Synergistic effect puts rare, specialized species at greater risk of extinction. Ecology 85:265–271.

Derocher, A.E., N.J. Lunn, and I. Stirling. 2004. Polar bears in a warming climate. Integrative and Comparative Biology 44:163–176.

_____, and M. Taylor. 1994. Density-dependent population regulation of polar bears. Pages 25-37 in M. Taylor (Editor). Density-Dependent Population Regulation of Black, Brown, and Polar Bears. 9th International Conference on Bear Research and Management, Monograph 3.

DeWeaver, E. 2007. Uncertainty in Climate Model Projections of Arctic Sea Ice Decline: An Evaluation Relevant to Polar Bears. USGS Alaska Science Center, Anchorage, Administrative Report.

Dunton, K.H., J.L. Goodall, S.V. Schonberg, J.M. Grebmeier, and D.R. Maidment. 2005. Multi-decadal synthesis of benthic–pelagic coupling in the western arctic: Role of cross-shelf advective processes. Deep-Sea Research II 52:3462–3477.

Durner, G.M., and S.C. Amstrup. 1995. Mass and body-dimension relationships of polar bears in northern Alaska. Wildlife Society Bulletin 24:480–484.

_____, _____, R. Nielson, T. McDonald. 2004. Using discrete choice modeling to generate resource selection functions for female polar bears in the Beaufort Sea. Pages 107–120 in S. Huzurbazar (Editor). Resource Selection

Methods and Applications: Proceedings of the 1st International Conference on Resource Selection, 13–15 January 2003, Laramie, Wyoming.

_____, D.C. Douglas, R.M. Nielson, and S.C. Amstrup. 2006. Model for Autumn Pelagic Distribution of Adult Female Polar Bears in the Chukchi Seas, 1987–1994. USGS Alaska Science Center, Anchorage, Final Report to USFWS.

Fancy, S.G., L.F. Pank, D.C. Douglas, C.H. Curby, G.W. Garner, S.C. Amstrup, and W.L. Regelin. 1988. Satellite telemetry: A new tool for wildlife research and management. USFWS, Washington, D.C., Resource Publication 172.

Ferguson, S.H., M.K. Taylor, and F. Messier. 1997. Space use by polar bears in and around Auyuittuq National Park, Northwest Territories, during the ice-free period. Canadian Journal of Zoology 75:1585–1594.

_____, _____, and _____. 2000. Influence of sea ice dynamics on habitat selection by polar bears. Ecology 81:761–772.

Fischbach, A.S., S.C. Amstrup, and D.C. Douglas. 2007. Landward and eastward shift of Alaskan polar bear denning associated with recent sea ice changes. Polar Biology:in press.

Garner, G.W., S.T. Knick, and D.C. Douglas. 1990. Seasonal movements of adult female polar bears in the Bering and Chukchi Seas. International Conference on Bear Research and Management 8:216–226.

Gjertz, I., K. M. Kovacs, C. Lydersen, and Ø. Wiig. 2000. Movements and diving of bearded seal (Erignathus barbatus) mothers and pups during lactation and post-weaning. Polar Biology. 23:559–566.

Hansen, J., M. Sato, R. Ruedy, K. Lo, D.W. Lea, and M. Medina-Elizade. 2006. Global temperature change. Proceedings of the

National Academy of Sciences 103:14,288–14,293.

Harwood, L.A., and I Stirling. 1992. Distribution of ringed seals in the southeastern Beaufort Sea during late summer. Canadian Journal of Zoology 70:891–900.

Holland, M.M., C.M. Bitz, and B. Tremblay. 2006. Future reductions in the summer Arctic sea ice. Geophysical Research Letters. 33:L23503.

Jakobsson, M., N.Z. Cherkis, J. Woodward, R. Macnab, and B. Coakley. 2000. New grid of Arctic bathymetry aids scientists and mapmakers. Eos 81(9):89.

Johnson, C.J., S.E. Nielson, E.H. Merrill, T.L. McDonald, and M.S. Boyce. 2006. Resource selection functions based on use-availability data: theoretical motivation and evaluation methods. Journal of Wildlife Management 70:347–357.

Keating, K.A., W.G. Brewster, and C.H. Key. 1991. Satellite telemetry: Performance of animal-tracking systems. Journal of Wildlife Management 55:160–171.

Kuhfeld, W.F. 2000. Multinomial Logit, Discrete Choice Modeling: An Introduction to Designing Choice Experiments, and Collecting, Processing, and Analyzing Choice Data with the SAS System. SAS Institute, Cary, North Carolina, Technical Report TS-621.

Kwok, R., G.F. Cunningham, and S.S. Pang. 2004. Fram Strait sea ice outflow. Journal of Geophysical Research 109:C01009.

Macdonald, R.W., and J.M. Bewers. 1996. Contaminants in the Arctic marine environment: priorities for protection. ICES Journal of Marine Sciences 53:537-563.

Manly, B.F.J., L.L. McDonald, D.L. Thomas, T.L. McDonald, and W.P. Erickson. 2002. Resource Selection by Animal Statistical Design and Analysis for Field Studies. Kluwer Academic Publishers, Dordrecht, Netherlands, 2nd edition.

Maslanik, J.A., S. Drobot, C. Fowler, W. Emery, and R. Barry. 2007. On the Arctic climate paradox and the continuing role of atmospheric circulation in affecting sea ice conditions. Geophysical Research Letters 34:L03711.

Mauritzen, M., S.E. Belikov, A.N. Boltunov, A.E. Derocher, E. Hanson, R.A. Ims, Ø. Wiig, and N. Yoccoz. 2003a. Functional responses in polar bear habitat selection. Oikos 100:112–124.

_____, A.E. Derocher, O. Pavlova, and Ø. Wiig. 2003b. Female polar bears, *Ursus maritimus*, on the Barents Sea drift ice: Walking the treadmill. Animal Behavior 66:107–113.

_____, _____, and Ø. Wiig. 2001. Space-use strategies of female polar bears in a dynamic sea ice habitat. Canadian Journal of Zoology 79:1704–1713.

_____, _____, _____, S.E. Belikov, A.N. Boltunov, E. Hansen, and G.W. Garner. 2002. Using satellite telemetry to define spatial population structure in polar bears in the Norwegian and western Russian Arctic. Journal of Applied Ecology 39:79–90.

McCracken, M.L., B.J.F. Manly, and M. Vander Heyden. 1998. Use of discrete-choice models for evaluating resource selection. Journal of Agricultural, Biological, and Environmental Statistics 3:268–279.

McLoughlin, P.D., M.S. Boyce, T. Coulson, and T. Clutton-Brock. 2006. Lifetime reproductive success and density-dependent, multi-variable resource selection. Proceedings of the Royal Society B 273:1449–1454.

Meier, W.N., J. Stroeve, and F. Fetterer. 2007. Whither Arctic sea ice? A clear signal of decline regionally, seasonally and extending

beyond the satellite record. Annals of Glaciology 46:428–434.

Monnett, C., and J.S. Gleason. 2006. Observations of mortality associated with extended open-water swimming by polar bears in the Alaskan Beaufort Sea. Polar Biology 29:681–687.

Ogi, M., and J.M. Wallace. 2007. Summer minimum Arctic sea ice extent and the associated summer atmospheric circulation. Geophysical Research Letters 34:L12705.

Ramsay, M.A., and K.A. Hobson. 1991. Polar bears make little use of terrestrial food webs: Evidence from stable-carbon isotope analysis. Oecologica 86:598–600.

_____, and I. Stirling. 1990. Fidelity of female polar bears to winter-den sites. Journal of Mammalogy 71:233–236.

Raynor, N.A., D.E. Parker, E.B. Horton, C.K. Folland, V.L. V. Alexander, and D.P. Rowell. 2003. Global analyses of sea surface temperature, sea ice, and night marine air temperature since the late nineteenth century. Journal of Geophysical Research 108(D14):4407.

Regehr, E.V., N.J. Lunn, S.C. Amstrup, and I. Stirling. 2007. Effects of earlier sea ice breakup on survival and population size of polar bears in western Hudson Bay. Journal of Wildlife Management. 71(8):in press.

Rigor, I.G., and J.M. Wallace. 2004. Variations in the age of Arctic sea-ice and summer sea-ice extent. Geophysical Research Letters 31: L09401.

_____, _____, and R.L. Colony. 2002. Response of sea ice to the Arctic Oscillation. Journal of Climate 15:2648–2663.

Rothrock, D.A., Y. Yu, and G.A. Maykut. 1999. Thinning of the Arctic sea-ice cover. Geophysical Research Letters 26:3469–3472.

Solomon, S., D. Qin, M. Manning, Z. Chen, M. Marquis, K.B. Averyt, M. Tignor, and H.L. Miller (Editors). 2007. Summary for policymakers. In Climate Change 2007: The Physical Science Basis. Contribution of Working Group I to the 4th Assessment Report of the Intergovernmental Panel on Climate Change (IPCC). Cambridge University Press, United Kingdom. Available from *http://www.ipcc.ch/*.

Stirling, I. 1997. Importance of polynyas, ice edges, and leads to marine mammals and birds. Journal of Marine Systems 10:9–21.

_____, D. Andriashek, and W. Calvert. 1993. Habitat preferences of polar bears in the western Canadian Arctic in late winter and spring. Polar Record 29:13–24.

_____, and W.R. Archibald. 1977. Aspects of predation of seals by polar bears. Journal of the Fisheries Research Board of Canada 34:1126–1129.

_____, and N.A. Oritsland. 1995. Relationships between estimates of ringed seal (*Phoca hispida*) and polar bear (*Ursus maritimus*) populations in the Canadian Arctic. Canadian Journal of Fisheries and Aquatic Science 52:2594–2612.

_____, and C.L. Parkinson. 2006. Possible effects of a warming climate on selected populations of polar bears (*Ursus maritimus*) in the Canadian Arctic. Arctic 59:261–275.

_____, C. Spencer, and D. Andriashek. 1989. Immobilization of polar bears (*Ursus maritimus*) with Telazol®. Journal of Wildlife Diseases 25:159–168.

Stroeve J., M.M. Holland, W. Meier, T. Scambos, and M. Serreze. 2007. Arctic sea ice decline: Faster than forecast. Geophysical Research Letters 34:L09501.

_____, M.C. Serreze, F. Fetterer, T. Arbetter, W. Meier, J. Maslanik, and K. Knowles. 2005.

Tracking the Arctic's shrinking ice cover: Another extreme September minimum in 2004. Geophysical Research Letters 32:L04501.

Taylor, M.K., S. Akeeagok, D. Andriashek, W. Barbour, E.W. Born, W. Calvert, H.D. Cluff, S. Ferguson, J. Laake, A. Rosing-Asvid, I. Stirling, and F. Messier. 2001. Delineating Canadian and Greenland polar bear (*Ursus maritimus*) populations by cluster analysis. Canadian Journal of Zoology 79:690–709.

Thiemann, G.W., S.J. Iverson, and I. Stirling. 2005. Seasonal, sexual and anatomical variability in the adipose tissue of polar bears (*Ursus maritimus*). Journal of Zoology 269:65–76.

Tucker, W.B., J.W. Weatherly, D.T. Eppler, L.D. Farmer, and D.L. Bentley. 2001. Evidence for rapid thinning of sea ice in the western Arctic Ocean at the end of the 1980s. Geophysical Research Letters 28:2851–2854.

USFWS. 2007. Endangered and Threatened Wildlife and Plants; 12-Month Petition Finding and Proposed Rule to List the Polar Bear (*Ursus maritimus*) as Threatened Throughout Its Range. Federal Register 72(5):9 January 2007.

Viranta. S. 2003. Geographic and temporal ranges of middle and late Miocene carnivores. Journal of Mammalogy 84:1267–1278.

Wadhams, P. 2000. Ice in the Ocean. Gordon and Breach Science Publishers, Amsterdam, Netherlands.

Wilcove, D.S., D. Rothstein, J. Dubow, A. Phillips, and E. Losos. 1998. Quantifying threats to imperiled species in the United States. Bioscience 48:607–615.

Woodgate, R.A., K. Aagaard, and T.J. Weingartner. 2006. Interannual changes in the Bering Strait fluxes of volume, heat and freshwater between 1991 and 2004. Geophysical Research Letters. 33:L15609.

Zhang, X., and J.E. Walsh. 2006. Toward a seasonally ice-covered Arctic Ocean: Scenarios from the IPCC AR4 model simulations. Journal of Climate 19:1730–1747.

Table 1. Ten IPCC AR-4 GCMs from which sea ice simulations and projections were extracted to define ice covariates for polar bear RSF models.

Includes IPCC model ID, country of origin, abbreviation used in this paper, approximate grid resolution (degrees), forcing scenario, and the number of runs used for the polar bear studies.

MODEL ID	Country	Acronym (this paper)	Grid Res. (lat x lon)	Forcing Scenario	Runs (n)
ncar_ccsm3_0	USA	CCSM3	1.0 x 1.0	20c3m	8
				SRES A1B	8
				SRES B1	8
cccma_cgcm3_1	Canada	CGCM3 T47	3.8 x 3.8	20c3m	1
				SRES A1B	1
cnrm_cm3	France	CNRM CM3	1.0 x 2.0	20c3m	1
				SRES A1B	1
gfdl_cm2_0	USA	GFDL CM2	0.9 x 1.0	20c3m	1
				SRES A1B	1
giss_aom	USA	GISS AOM	3.0 x 4.0	20c3m	1
				SRES A1B	1
ukmo_hadgem1	UK	HadGEM1	0.8 x 1.0	20c3m	1
				SRES A1B	1
ipsl_cm4	France	IPSL CM4	1.0 x 2.0	20c3m	1
				SRES A1B	1
miroc3_2_medres	Japan	MIROC32	1.0 x 1.4	20c3m	1
				SRES A1B	1
miub_echo_g	Germany/Korea	MIUB ECHO	1.5 x 2.8	20c3m	1
				SRES A1B	1
mpi_echam5	Germany	MPI ECHAM5	1.0 x 1.0	20c3m	1
				SRES A1B	1

Table 2. Candidate *a priori* models for a polar bear Resource Selection Function in the pelagic region of the Arctic, 1985–1995.

Model Num.	Model	Season
1	*totcon*	all
2	*totcon + bathymetry*	all
3	*totcon + dist2land*	all
4	*totcon + dist15*	all
5	*totcon + dist50*	all
6	*totcon + dist75*	all
7	*totcon + bathymetry + dist2land*	all
8	*totcon + bathymetry + dist15*	all
9	*totcon + bathymetry + dist50*	all
10	*totcon + bathymetry + dist75*	all
11	*totcon + dist2land + dist50*	spring, summer
12	*totcon + dist2land + dist75*	spring, summer, autumn
13	*totcon + dist15 + dist50*	summer
14	*totcon + dist15 + dist75*	spring, summer, autumn
15	*totcon + dist50 + dist75*	spring, summer
16	$totcon + totcon^2$	all
17	$totcon + totcon^2 + bathymetry$	all
18	$totcon + totcon^2 + dist2land$	all
19	$totcon + totcon^2 + dist15$	all
20	$totcon + totcon^2 + dist50$	all
21	$totcon + totcon^2 + dist75$	all
22	$totcon + totcon^2 + bathymetry + dist2land$	all
23	$totcon + totcon^2 + bathymetry + dist15$	all
24	$totcon + totcon^2 + bathymetry + dist50$	all
25	$totcon + totcon^2 + bathymetry + dist75$	all
26	$totcon + totcon^2 + dist2land + dist50$	spring, summer
27	$totcon + totcon^2 + dist2land + dist75$	spring, summer, autumn
28	$totcon + totcon^2 + dist15 + dist50$	summer
29	$totcon + totcon^2 + dist15 + dist75$	spring, summer, autumn
30	$totcon + totcon^2 + dist50 + dist75$	spring, summer

Table 3. Numbers of polar bear locations in pelagic IUCN units by year used for estimating (1985–1995) and evaluating (1996–2006) Resource Selection Functions (RSF).

RSF building (1985–1995)

IUCN Unit	1985	1986	1987	1988	1989	1990	1991	1992	1993	1994	1995	Total
Chukchi Sea	3	184	301	375	343	892	603	648	694	270	-	4,313
S. Beaufort Sea	87	302	326	495	677	283	332	709	403	148	-	3,762
Laptev Sea	-	3	-	23	404	415	167	249	322	52	7	1,642
Arctic Basin	8	96	143	67	302	228	36	116	221	148	7	1,372
Barents Sea	-	-	-	-	15	6	89	103	101	95	109	518
N. Beaufort Sea	-	-	-	11	2	16	6	37	109	116	-	297
E. Greenland	-	-	-	-	-	-	-	3	35	38	62	138
Kara Sea	-	-	-	-	-	-	31	37	-	61	-	129
Total	98	585	770	971	1,743	1,840	1,264	1,902	1,885	928	185	12,171

RSF evaluation (1996–2006)

IUCN Unit	1996	1997	1998	1999	2000	2001	2002	2003	2004	2005	2006	Total
Chukchi Sea	-	-	9	4	3	49	7	21	37	50	43	223
S. Beaufort Sea	-	77	95	290	623	734	616	366	584	776	532	4,693
Laptev Sea	-	-	-	-	-	-	-	-	-	-	-	-
Arctic Basin	-	12	69	76	19	36	42	32	179	303	196	964
Barents Sea	84	95	86	169	-	-	-	-	-	-	-	434
N. Beaufort Sea	-	-	5	10	247	216	335	133	261	67	43	1,317
E. Greenland	32	19	9	-	-	-	-	-	-	-	-	60
Kara Sea	-	39	-	-	-	-	-	-	-	-	-	39
Total	116	242	273	549	892	1,035	1,000	552	1,061	1,196	814	7,730

Table 4. Data distribution of individual polar bears and number of used locations, used to build a polar bear resource selection function for the pelagic realm of the Arctic, 1985–1995.

Location data from most bears occurred in more than one season.

Season	Number of individuals	Number of used locations
Winter	322	5488
Spring	292	3408
Summer	237	1650
Autumn	216	1625
Total	N/A	12,171

Table 5. Data distribution of individual polar bears, number of used locations, and number of available locations by jurisdictional origin, used to build and evaluate a polar bear resource selection function for the pelagic realm of the Arctic, 1985–2006.

Region	Number of individuals	Number of used locations	Number of available locations
1985–1995: model building			
Norway	47	519	43,816
United States	250	10,085	1,141,745
Canada	28	1433	110,429
Denmark	8	134	14,815
Total	333	12,171	1,310,805
1996–2006: model evaluation			
Norway	45	413	48,591
United States	105	5870	509,128
Canada	18	1387	157,439
Denmark	2	60	7247
Total	170	7730	722,405

Table 6. Pearson correlation matrix of covariates used for a polar bear resource selection function in the pelagic realm of the Arctic, 1985–1995.

Significant correlations are shaded in gray.

Season	Variable 1	Variable 2					
		TOTCON	DIST2LAND	BATH	DIST15	DIST50	DIST75
Winter	TOTCON	1					
	DIST2LAND	0.015	1				
	BATH	0.082	0.443	1			
	DIST15	0.200	0.763	0.234	1		
	DIST50	0.208	0.778	0.249	0.975	1	
	DIST75	0.158	0.753	0.266	0.948	0.977	1
Spring	TOTCON	1					
	DIST2LAND	0.125	1				
	BATH	0.204	0.365	1			
	DIST15	0.427	0.656	0.234	1		
	DIST50	0.252	0.512	0.214	0.812	1	
	DIST75	-0.391	0.232	0.023	0.236	0.480	1
Summer	TOTCON	1					
	DIST2LAND	0.350	1				
	BATH	0.405	0.344	1			
	DIST15	0.520	0.609	0.401	1		
	DIST50	-0.097	0.209	0.027	0.585	1	
	DIST75	-0.537	-0.176	-0.184	-0.040	0.515	1
Autumn	TOTCON	1					
	DIST2LAND	0.162	1				
	BATH	0.254	0.424	1			
	DIST15	0.342	0.708	0.303	1		
	DIST50	0.307	0.600	0.375	0.751	1	
	DIST75	-0.095	0.396	0.264	0.442	0.754	1

Table 7. Coefficients and standard errors of covariates in the top model for each season for Resource Selection Functions for polar bears in the polar basin.

Standard errors (in parentheses) were calculated by bootstrapping (replicates = 2,000) individual bears.

Season	*totcon*	*totcon²*	*bath*	*dist2land*	*dist15*
Winter	0.08602 (0.01856)	-0.00046 (0.00012)	-0.00037 (0.00006)	-0.00474 (0.00047)	-
Spring	0.06551 (0.00409)	-0.00040 (0.00004)	-0.00020 (0.00005)	-	-0.00261 (0.00050)
Summer	0.04676 (0.00582)	-0.00037 (0.00007)	-0.00017 (0.00005)	-	-0.00436 (0.00083)
Autumn	0.08130 (0.00635)	-0.00068 (0.00006)	-0.00025 (0.00005)	-	-0.00604 (0.00054)

Table 8. Average rates of change (% / decade) in the annual cumulative area of optimal polar bear habitat based on sea ice projections by 10 IPCC AR-4 general circulation models, and their ensemble mean.

Rates of change (% / decade) were calculated from estimates of slope (total area / year) based on linear regression analysis with the annual cumulative area of optimal habitat as the dependent variable, and year as the independent variable. Fonts denote statistical significance of estimates of % change: $P < 0.01$ **bold underline**; $P < 0.05$ **bold**; $P < 0.10$ underline; and $P > 0.10$ gray. All GCMs were forced with the IPCC SRES-A1B scenario, and results for CCSM3 under the SRES-B1 scenario are additionally shown. For comparison, the rate of optimal habitat change based on satellite observations of sea ice during 1979–2006, is shown in parentheses below each IUCN heading. To help gauge relative sizes of areas of optimal sea ice in each IUCN during 1979–2006, the mean annual cumulative area (km2) of optimal habitat during 1979–2006 is in brackets.

IUCN	Period	Ensemble	ccsm3 a1b	ccsm3 b1	cgcm3	cnrm	gfdl	giss	hadgem	ipsl	miroc	miub	mpi
Full Study Area													
	2001-2099	-4.0	-4.9	-2.7	-2.4	-3.5	-2.4	-1.5	-5.3	-3.1	-5.7	-2.9	-6.7
(-5.0)	2001-2050	-3.7	-6.2	-4.0	-2.6	-3.2	-1.4	-3.3	-4.3	-4.7	-3.0	-1.7	-6.6
[1,464,000]	2050-2075	-6.1	-4.7	-3.3	0.8	-4.3	-5.8	0.2	-9.4	-4.3	-10.8	-4.9	-16.8
	2075-2099	-3.1	-2.7	-1.0	-1.7	-4.1	-0.7	1.9	-10.8	4.3	-11.5	-5.1	-2.6
Canada/Grnland													
	2001-2099	-3.0	-3.4	-1.5	-1.7	-2.6	-1.6	-0.6	-3.4	-2.3	-5.0	-1.5	-5.9
(-4.0)	2001-2050	-2.7	-3.8	-2.4	-1.5	-2.8	-1.0	-1.0	-2.5	-3.0	-3.0	-0.2	-5.8
[453,000]	2050-2075	-4.2	-3.7	-2.7	-0.2	-2.5	-4.2	-1.2	-7.5	3.5	-10.3	-3.4	-10.8
	2075-2099	-2.6	-2.3	0.2	2.6	-4.4	-0.8	1.8	-10.6	-4.5	-6.3	1.5	-2.9
Alaska/Eurasia													
	2001-2099	-4.3	-5.8	-3.4	-2.7	-3.7	-2.7	-1.8	-6.1	-3.5	-5.9	-3.5	-7.1
(-5.5)	2001-2050	-4.2	-7.4	-4.9	-3.0	-3.4	-1.5	-4.0	-5.0	-5.5	-3.0	-2.3	-7.0
[1,011,000]	2050-2075	-7.0	-5.4	-3.6	1.2	-4.8	-6.4	0.7	-10.4	-8.2	-11.0	-5.6	-19.6
	2075-2099	-3.4	-2.9	-1.7	-3.5	-4.0	-0.7	1.9	-11.0	10.3	-13.5	-8.0	-2.4
Q. Elizabeth													
	2001-2099	-0.9	-2.0	-0.4	1.3	-1.7	0.0	1.2	-1.5	0.7	-3.3	0.5	-2.9
(-1.9)	2001-2050	0.7	-0.8	-0.4	1.7	-0.6	1.7	2.6	0.1	1.1	0.7	2.5	-1.0
[127,000]	2050-2075	-2.3	-3.4	-1.6	0.3	-4.1	-0.5	-1.0	-3.9	5.6	-10.4	-2.3	-3.3
	2075-2099	-2.2	-3.4	0.2	6.1	-5.9	-0.6	-0.8	-7.0	-1.8	-5.3	-0.2	-3.9
E. Greenland													
	2001-2099	-4.3	-4.2	-2.4	-2.2	-2.7	-2.3	-0.9	-5.2	-3.7	-6.6	-2.3	-8.1
(-7.7)	2001-2050	-4.8	-6.0	-4.3	-1.8	-2.7	-2.8	-2.8	-4.5	-4.0	-6.4	-2.9	-9.3
[193,000]	2050-2075	-5.1	-4.5	-1.6	-2.6	-1.5	-5.1	2.1	-12.2	2.5	-9.9	1.3	-15.0
	2075-2099	-2.9	-1.3	0.0	0.7	-4.7	-0.3	9.4	-14.0	-6.8	-10.4	9.0	-5.4

Table 8 (continued).

IUCN	Period	Ensemble	ccsm3 a1b	ccsm3 b1	cgcm3	cnrm	gfdl	giss	hadgem	ipsl	miroc	miub	mpi
Barents Sea													
	2001-2099	-6.5	-11.5	-8.0	-2.7	-5.8	-4.5	0.3	-11.5	-3.8	-10.1	-5.5	-10.9
(-10.7)	2001-2050	-5.9	-14.2	-11.3	-3.8	-3.8	-2.4	-4.5	-11.1	-3.2	-2.9	-1.1	-14.3
[131,000]	2050-2075	-13.1	-29.8	-15.6	4.0	-2.9	-9.5	-1.9	-30.6	-17.3	-31.0	-10.1	-34.2
	2075-2099	-0.3	-21.1	-9.6	-5.6	-9.2	7.0	7.1	-17.5	20.7	-42.7	-9.1	51.1
Kara Sea													
	2001-2099	-4.2	-5.1	-3.3	-1.5	-3.0	-2.6	-1.2	-6.8	-3.0	-6.8	-4.3	-8.8
(-5.1)	2001-2050	-3.3	-7.3	-4.5	-1.2	-2.1	-1.1	-1.9	-5.1	-2.6	-2.0	-2.1	-9.4
[291,000]	2050-2075	-6.7	-6.6	-3.3	4.4	0.1	-4.2	4.9	-13.9	-15.5	-15.9	-7.3	-20.8
	2075-2099	-2.6	-2.6	-1.0	-3.6	-3.1	-0.2	1.7	-13.0	15.8	-18.7	-9.3	6.2
Laptev Sea													
	2001-2099	-2.4	-4.0	-2.2	-1.0	-2.3	-1.3	-1.3	-4.1	-1.9	-2.3	-2.2	-3.9
(-1.9)	2001-2050	-2.3	-4.8	-2.4	-1.5	-0.8	-0.6	-3.1	-2.6	-6.0	-0.8	-1.9	-1.3
[309,000]	2050-2075	-4.1	-2.6	-0.4	0.5	-7.9	-3.5	0.3	-8.9	-0.2	-1.9	-2.1	-11.9
	2075-2099	-2.7	-2.4	-2.8	0.2	-2.4	-1.4	-0.8	-6.6	5.9	-4.7	-11.1	-1.7
Chukchi Sea													
	2001-2099	-5.3	-6.4	-3.4	-5.4	-5.1	-3.3	-4.2	-5.5	-6.0	-6.7	-2.2	-6.8
(-8.0)	2001-2050	-6.1	-8.1	-5.7	-6.0	-7.4	-2.2	-8.1	-4.1	-11.6	-6.5	-3.8	-6.0
[196,000]	2050-2075	-7.8	-4.2	-2.7	-3.5	-8.6	-9.5	-1.8	-5.6	20.3	-6.2	-1.8	-23.0
	2075-2099	-7.5	-2.0	-0.7	-8.7	-5.1	-3.8	3.8	-15.4	-5.6	-19.2	0.0	-14.4
S. Beaufort Sea													
	2001-2099	-5.2	-5.3	-2.7	-5.0	-4.5	-2.8	-4.4	-4.5	-9.8	-4.7	-3.7	-7.9
(-4.8)	2001-2050	-5.9	-6.6	-3.8	-4.0	-6.6	-2.3	-6.5	-5.3	-15.1	-4.0	-3.0	-8.3
[84,000]	2050-2075	-8.8	-4.0	-7.3	0.2	-3.9	-12.0	-7.4	-7.4	8.1	-9.6	-10.8	-24.0
	2075-2099	-4.2	-3.6	1.6	-3.3	-3.8	-1.8	0.3	-9.9	-15.2	-8.5	-5.3	5.4
N. Beaufort Sea													
	2001-2099	-3.5	-3.5	-1.4	-3.7	-3.5	-2.2	-2.3	-3.0	-3.7	-4.8	-2.4	-5.5
(-0.2)	2001-2050	-3.3	-3.2	-1.4	-3.7	-5.2	-1.1	-3.2	-2.7	-6.2	-2.7	-0.5	-4.7
[132,000]	2050-2075	-5.4	-2.5	-5.1	2.1	-1.4	-6.9	-3.8	-6.0	1.3	-10.6	-8.0	-14.5
	2075-2099	-2.8	-2.6	0.7	0.4	-2.0	-1.3	-0.5	-10.5	-6.7	-3.0	-1.2	1.1
Arctic Basin													
	2001-2099	1.6	-2.2	1.1	13.3	-4.1	3.7	2.7	12.1	10.8	-3.5	-2.9	0.4
(33.9)	2001-2050	12.9	3.3	3.3	3.8	-0.5	19.2	6.8	33.4	12.5	29.8	13.7	15.9
[2,000]	2050-2075	-0.9	-9.3	2.8	21.8	-22.0	-0.9	8.9	9.1	8.0	-15.0	-6.4	4.1
	2075-2099	-3.8	-9.0	-7.5	15.5	10.2	-16.8	1.3	-20.6	47.3	-15.7	-10.0	-9.4

Table 9. Regional assessment of RSF model performance for all seasons (pooled) and years (1985–2006) showing the proportion of polar bear locations within the top 20% and top 50% of the RSF-valued habitat.

The total monthly RSF habitat area of each region was independently partitioned into 20 equal-area RSF-value intervals prior to enumerating the within-interval bear frequencies.

Region	In the Top 20% RSF-valued Habitat	In the Top 50% RSF-valued Habitat	Number of polar bear locations
Full Study Area (i.e., Fig. 8)	76 %	97 %	19901
Alaska-Eurasia	67 %	90 %	14408
Canada-Greenland	87 %	99 %	5493
Arctic Basin	97 %	100 %	2308
Northern Beaufort Sea	77 %	99 %	2959
East Greenland	50 %	88 %	198
Queen Elizabeth	79 %	100 %	28
Southern Beaufort Sea	64 %	94 %	8455
Chukchi Sea	47 %	85 %	4536
Laptev Sea	47 %	75 %	297
Kara Sea	43 %	70 %	168
Barents Sea	72 %	87 %	952

Figure 1. The polar basin RSF study area, defined by a composite of IUCN polar bear subpopulation units located in the Arctic Ocean and peripheral seas (Pelagic Ecoregion).

Units are color-shaded to distinguish membership within 2 groups based on general sea ice dynamics: "Alaska-Eurasia" (purple) where divergent ice is generally advected offshore (and melts away from shore during summer); and "Canada-Greenland (cyan) where ice motion promotes convergence and shoreward drift year-round. Polar bears inhabit 2 other ecoregions (Archipelago and Seasonal) in northeast North America, but these regions were not part of our study area due to insufficient samples of polar bear tracking data and dramatically different sea ice characteristics. Barents Sea (BS), Kara Sea (KS), Laptev Sea (LVS), Chukchi Sea (CS), Southern Beaufort Sea (SBS), Northern Beaufort Sea (NBS), Arctic Basin (AB), Queen Elizabeth (QE), and East Greenland (EG); Kane Basin (KB), Norwegian Bay (NW), Viscount Melville Sound (VM), Lancaster Sound (LS), M'Clintock Channel (MC), and Gulf of Boothia (GB); Baffin Bay (BB), Davis Strait (DS), Foxe Basin (FB), Western Hudson Bay (WHB), and Southern Hudson Bay (SHB).
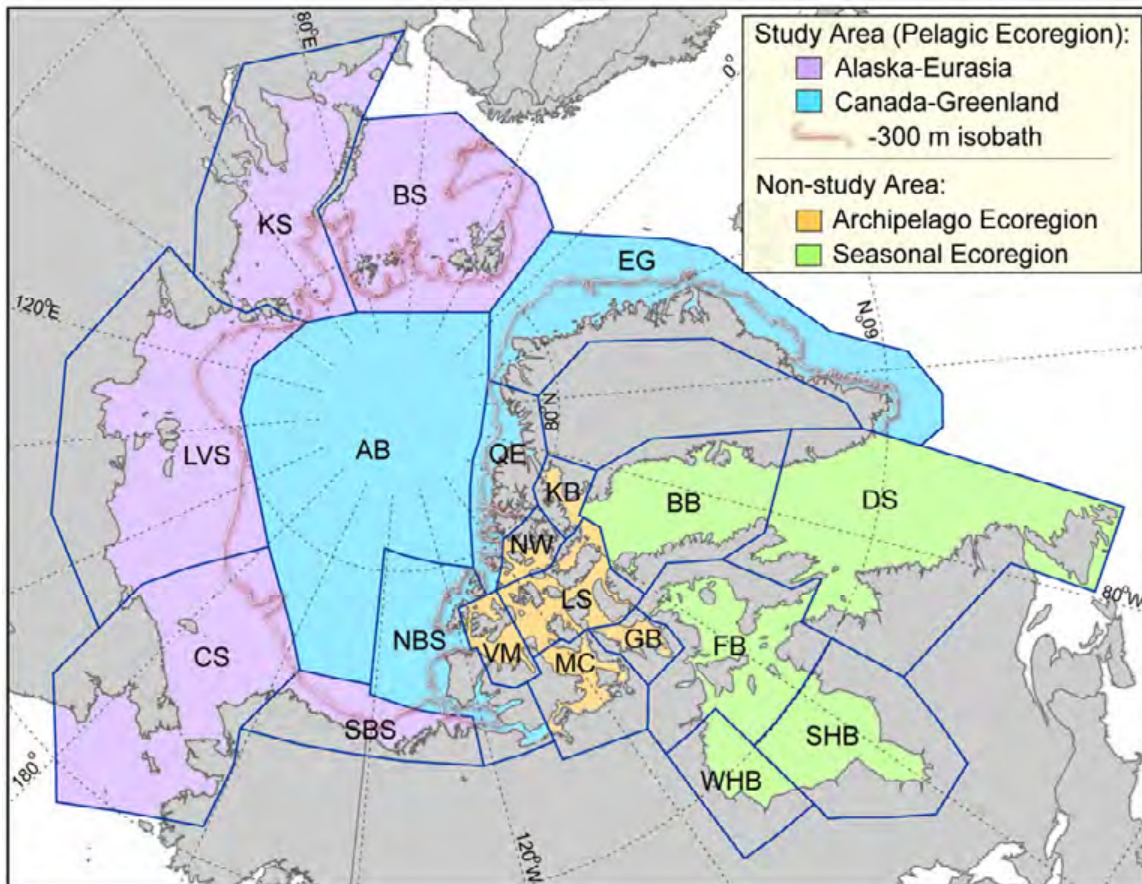
Figure 2. (a) Schematic of the algorithm used to classify months into one of four ice-seasons. (b) Example of the ice-season classification algorithm applied to projected sea ice extent during the 21st century by the CCSM3 GCM (run-1) and the SRES-A1B forcing scenario.

A month was assigned to the ice-maximum season if its proportional ice extent in the Arctic Ocean exceeded a threshold "t", as defined by the month of greatest ice extent minus 15% of the maximum annual amplitude of ice extent change from the previous or subsequent minimum extent. An inverse algorithm (not shown) was used to assign months to the ice-minimum season. Intervening months were assigned to either the ice-melt or ice-growth season depending on their chronology relative to the maximum and minimum.

Ice maximum season
if: $P_x > t$, where
$t = P_m - (0.15 \max[a_{y-1}, a_{y+1}])$

Ice Season:
• • • Maximum (winter)
• • • Melt (spring)
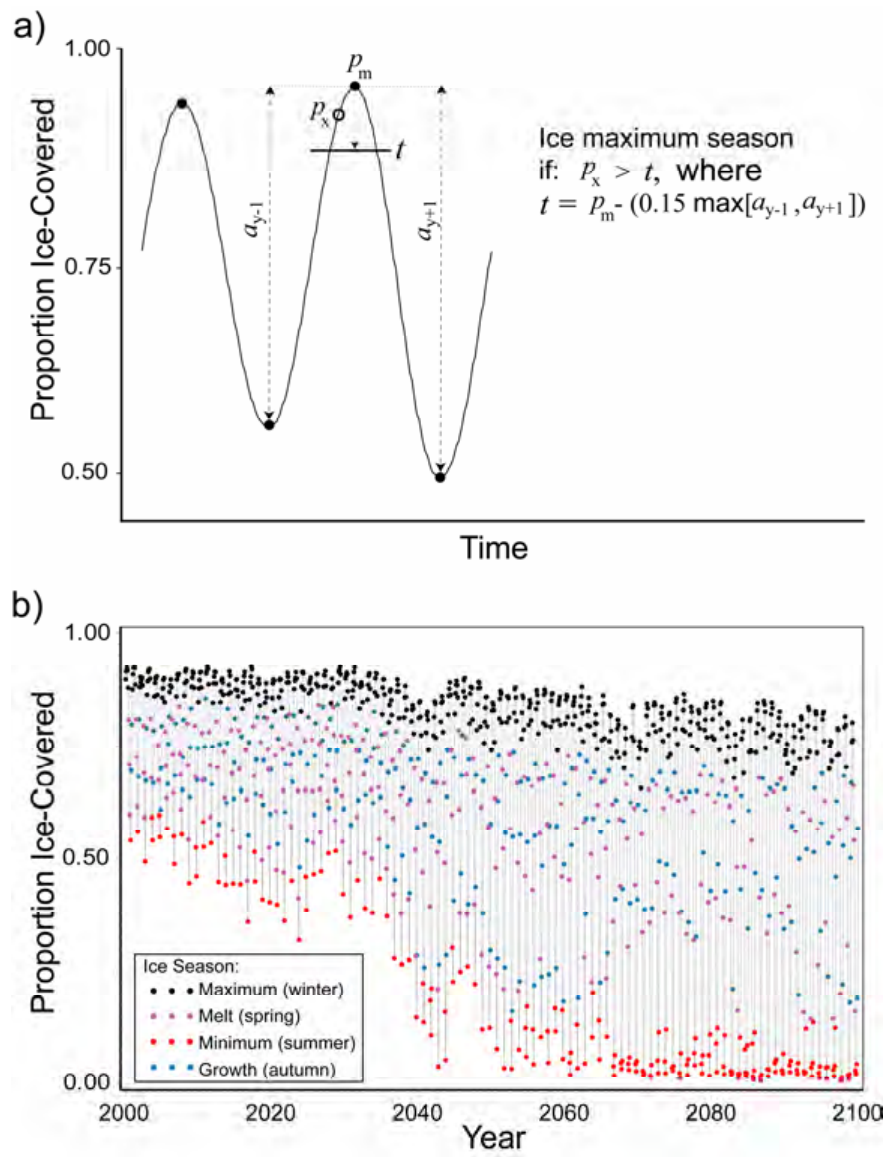• • • Minimum (summer)
• • • Growth (autumn)

Figure 3. Example of two consecutive locations of polar bear #20224 on 8 (yellow point) and 14 (red point) September 2005, and the probable extent of available habitat (red circle) had the bear sustained a maximum rate of travel for the 6 day period.
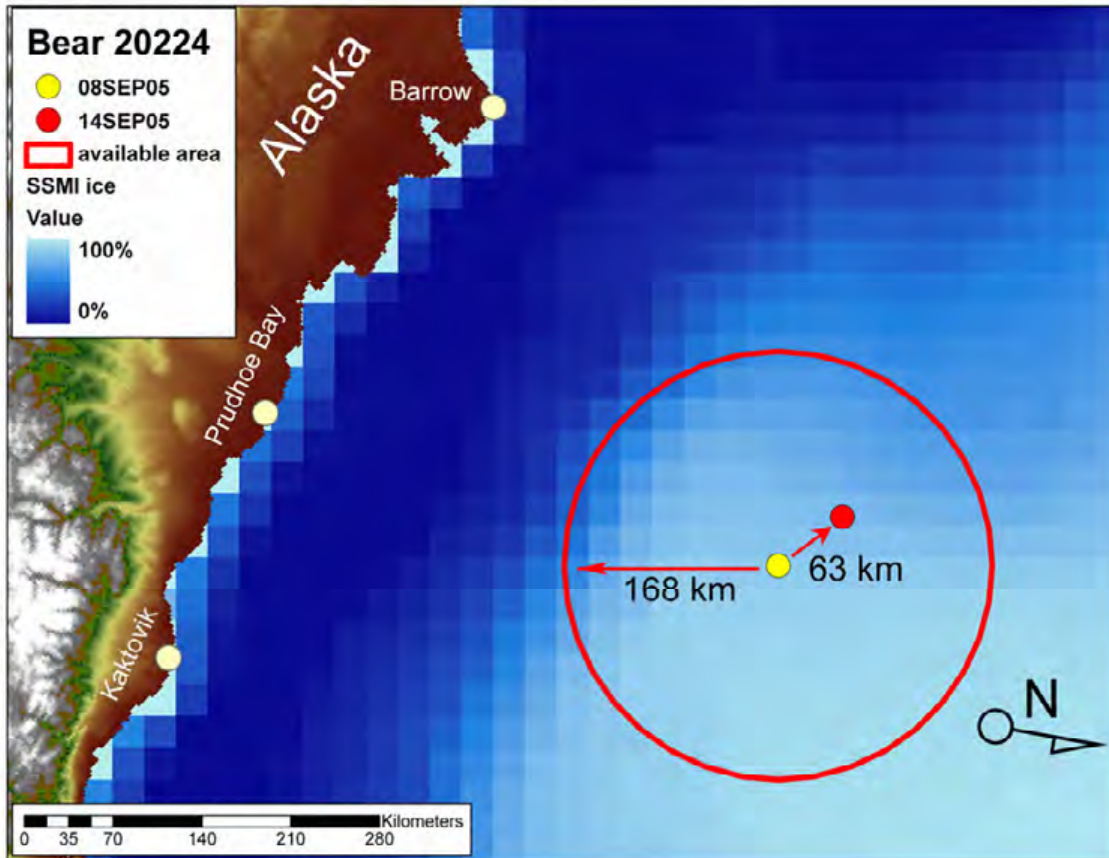
Figure 4. An example of habitat pixels available to a polar bear as it moved from one location (yellow point) to another location (red point and black pixel). All pixels within the red circle were considered available for selection by the bear but only the black pixel containing the second bear location (red point) was coded as a used point. Each pixel in the availability circle included *totcon*, *bath*, *dist2land*, *dist15*, *dist50*, and *dist75*.
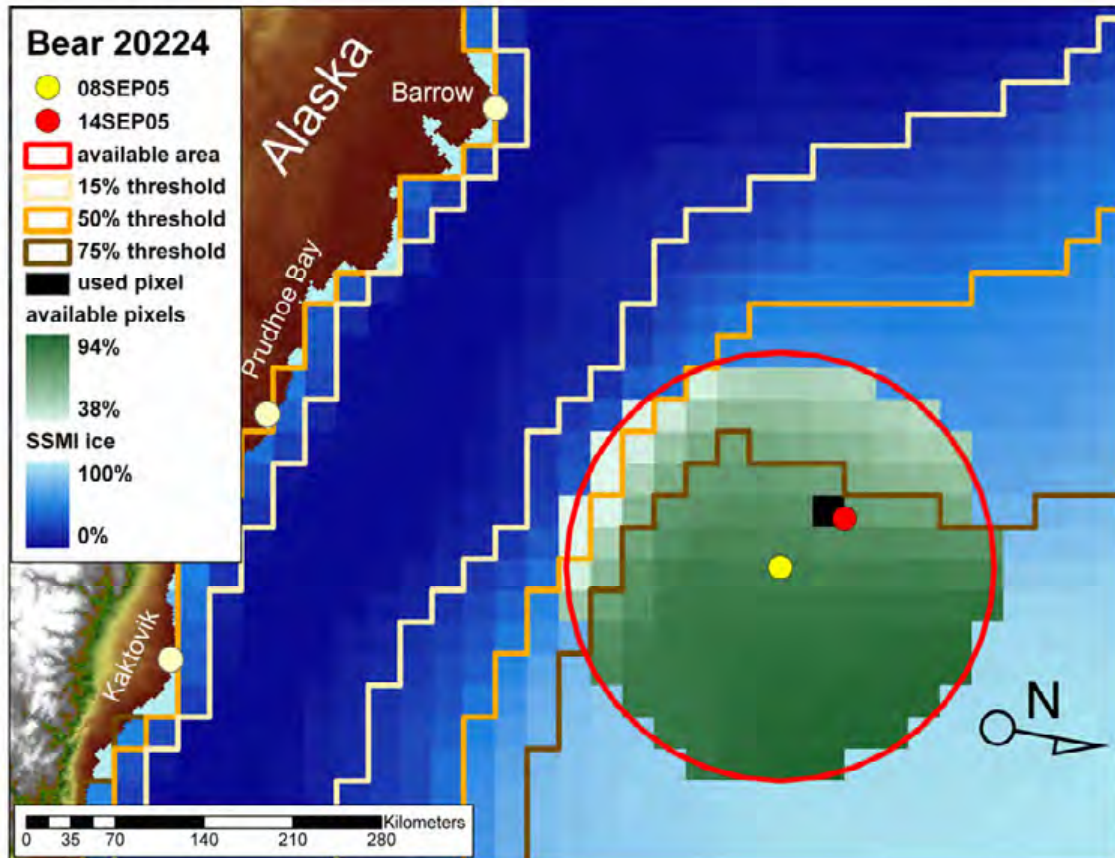
Figure 5. Distribution of all polar bear locations 1985–1995, by jurisdictional origin, used to build a polar bear RSF for the pelagic realm of the Arctic.
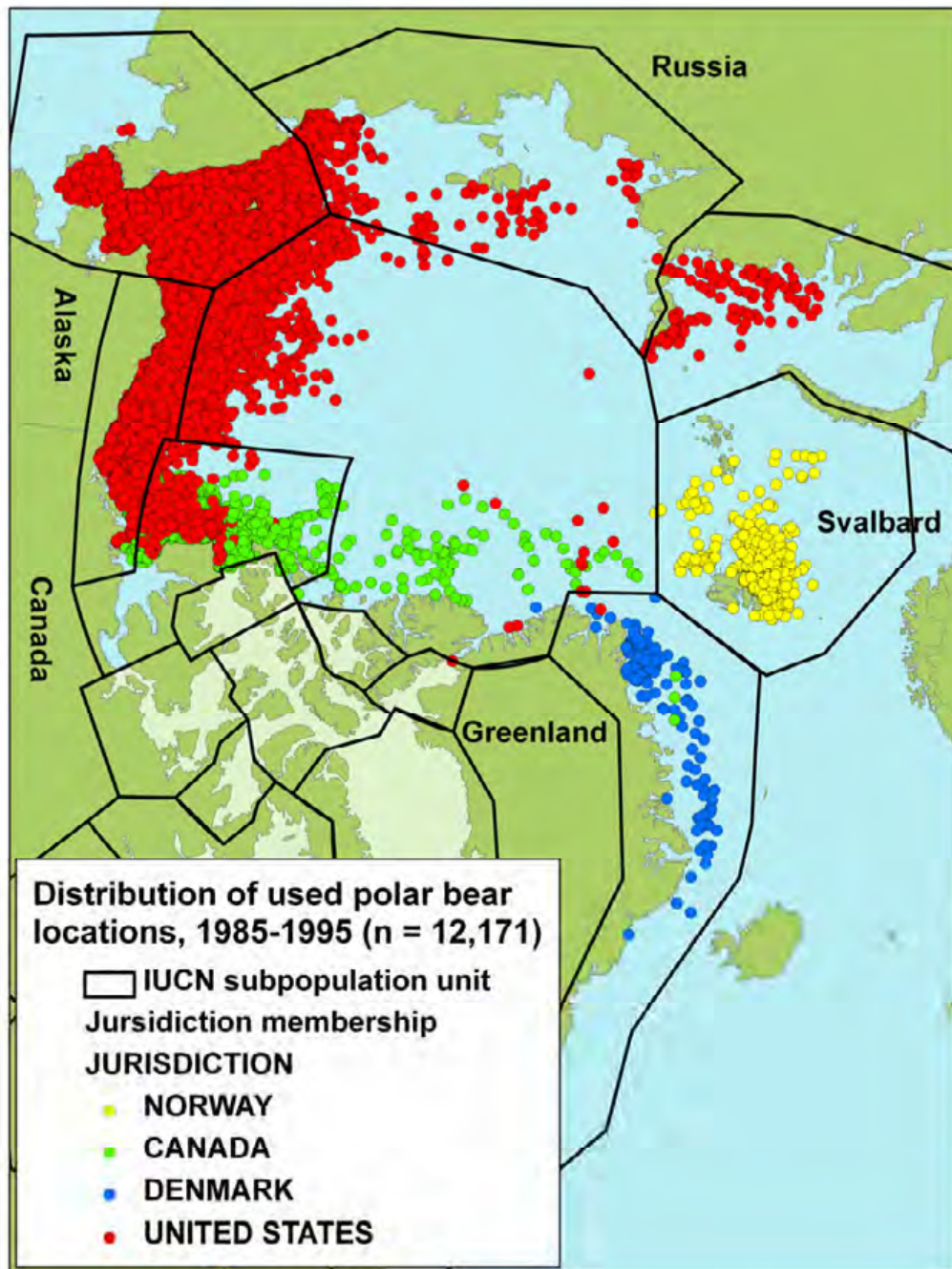
Figure 6. Ensemble mean season length of 10 GCMs used in this study (black, mean ± min/max) and the observed satellite record (red), where seasons were dynamically defined by the amplitude of annual ice growth and retreat (see Fig. 2).
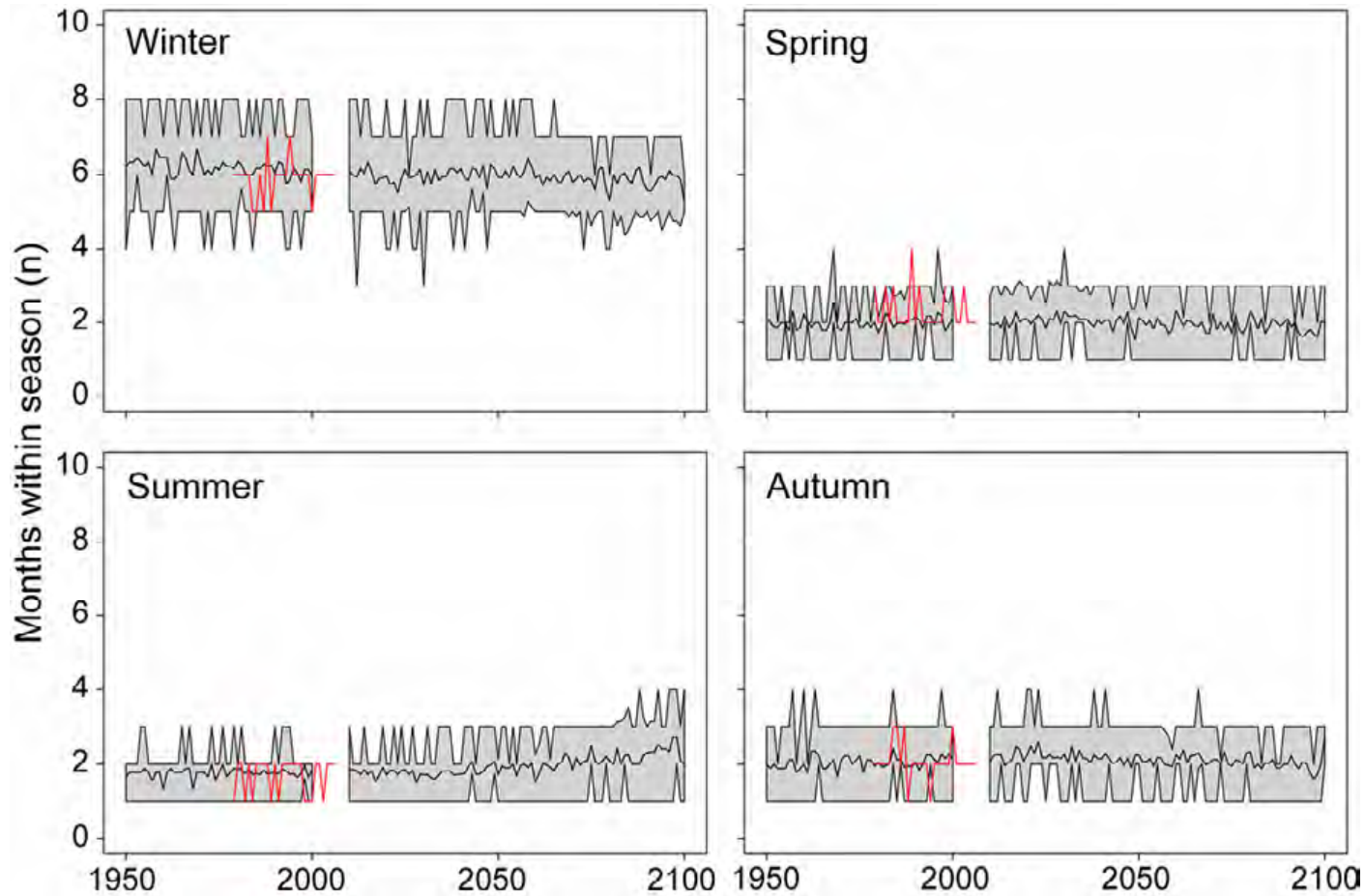
Figure 7. Responses of four covariates in the seasonal RSF models developed for polar bears in the pelagic realm of the Arctic, 1985–1995.

Variables not in plots were held at their median values. RSF predictions were scaled so the maximum prediction was 1.0 for each season.
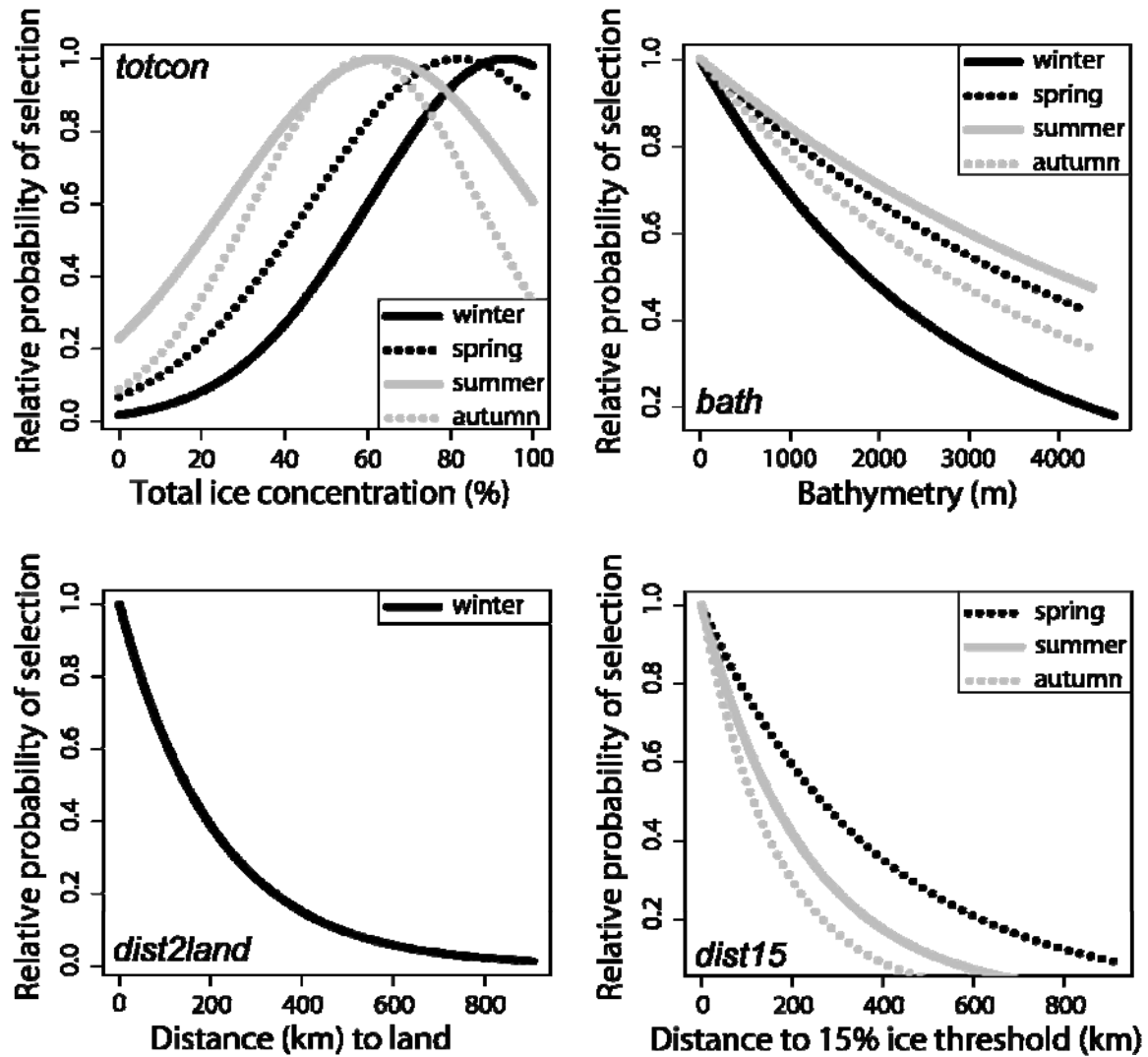
Figure 8. Proportions of polar bear tracking locations occupying 20 equal area intervals of the extrapolated monthly RSF maps (i.e. each 5% of the total monthly RSF habitat) along an increasing RSF-value gradient.

All locations (gray histograms and cumulative frequencies) are shown partitioned into the 1985–1995 period (light blue) that was used to estimate the RSF models, and the subsequent 1996–2006 period (red) when sea ice conditions were markedly different and tracking studies were conducted primarily in the Beaufort Sea. Histogram segments appear dark blue when the 1985–1995 and 1996–2006 proportions overlap.
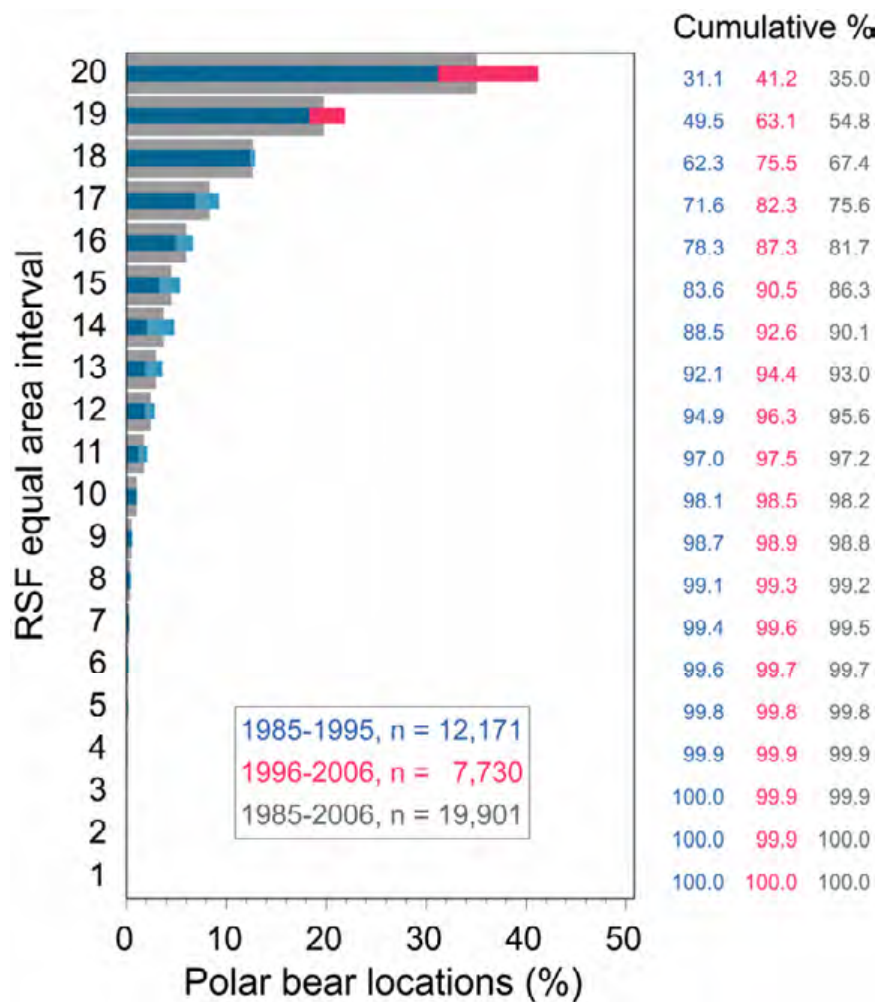
Figure 9a. Examples of monthly RSF-value habitat maps derived from satellite-observed sea ice data with (left) the summer RSF model and (right) the winter RSF model.

To represent a single month within the 1985–1995 period, the year-month with the smallest difference in ice extent compared to the decadal average was selected for illustration. 2005 is shown to illustrate observed changes in a recent record-breaking year of minimum summer ice extent.

9a)
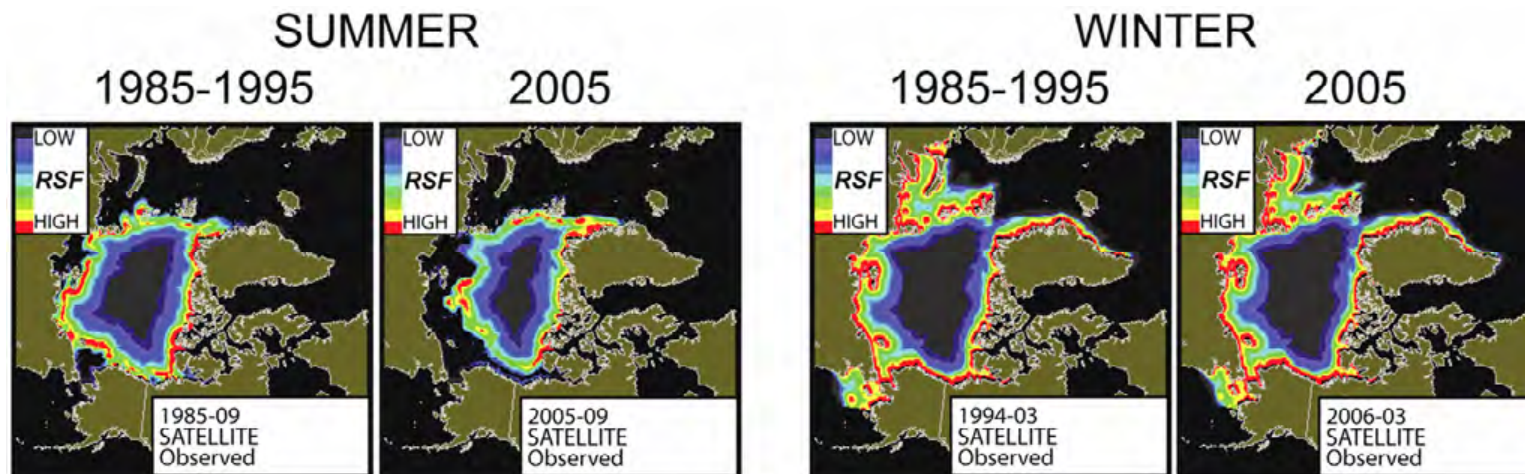
Figure 9b. Examples of monthly summer RSF-value habitat maps for the mid- and late-21st century derived with ice projections by 10 IPCC AR-4 GCMs (labeled in lower right corner of each panel) when forced with the SRES-A1B scenario.

To represent a decadal range of years, the year-month with the smallest difference in ice extent compared to the decadal average was selected for illustration.

9b)
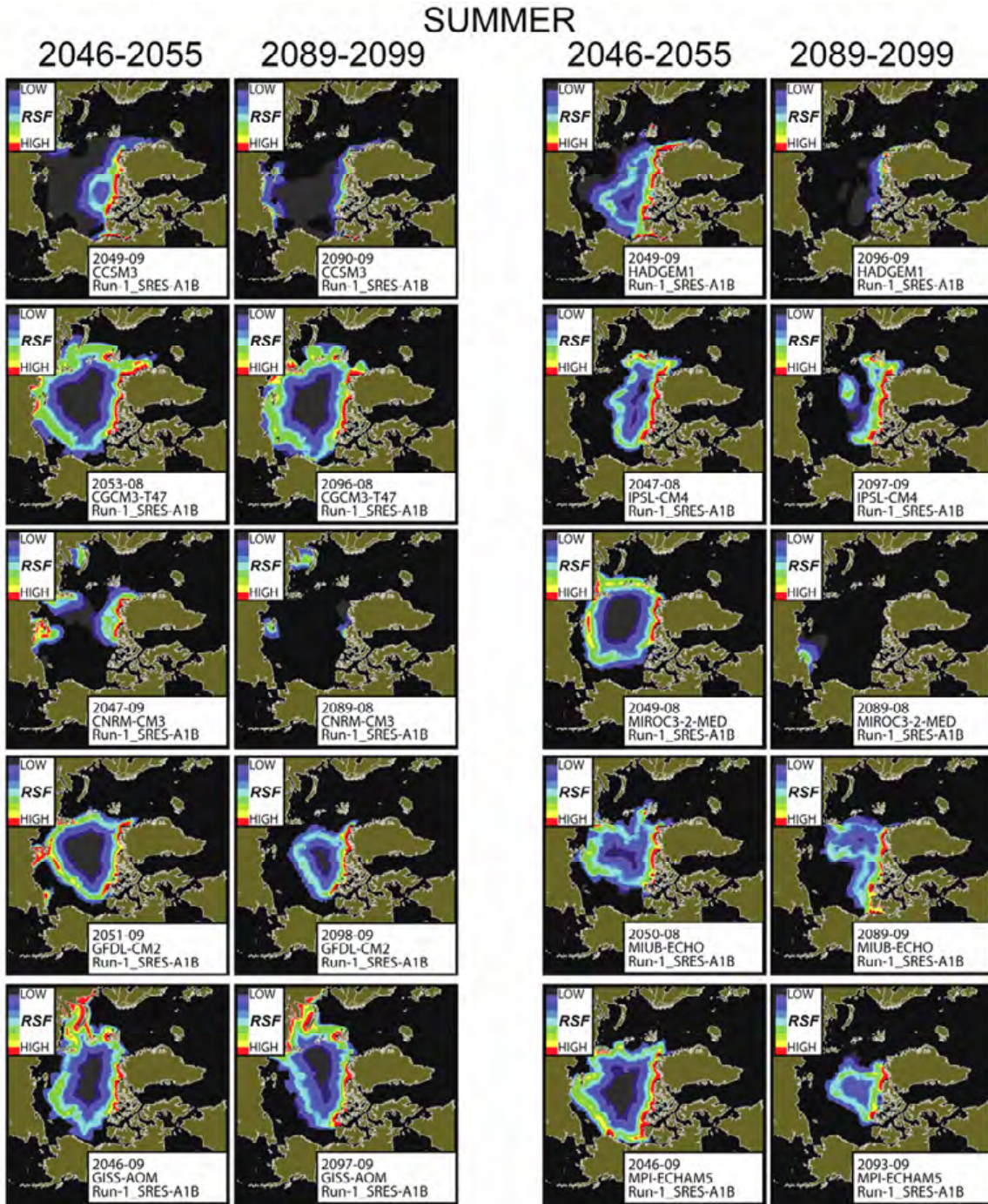
Figure 9c. Examples of monthly winter RSF-value habitat maps for the mid- and late-21st century derived with ice projections by 10 IPCC AR-4 GCMs (labeled in lower right corner of each panel) when forced with the SRES-A1B scenario.

To represent a decadal range of years, the year-month with the smallest difference in ice extent compared to the decadal average was selected for illustration.

9c)
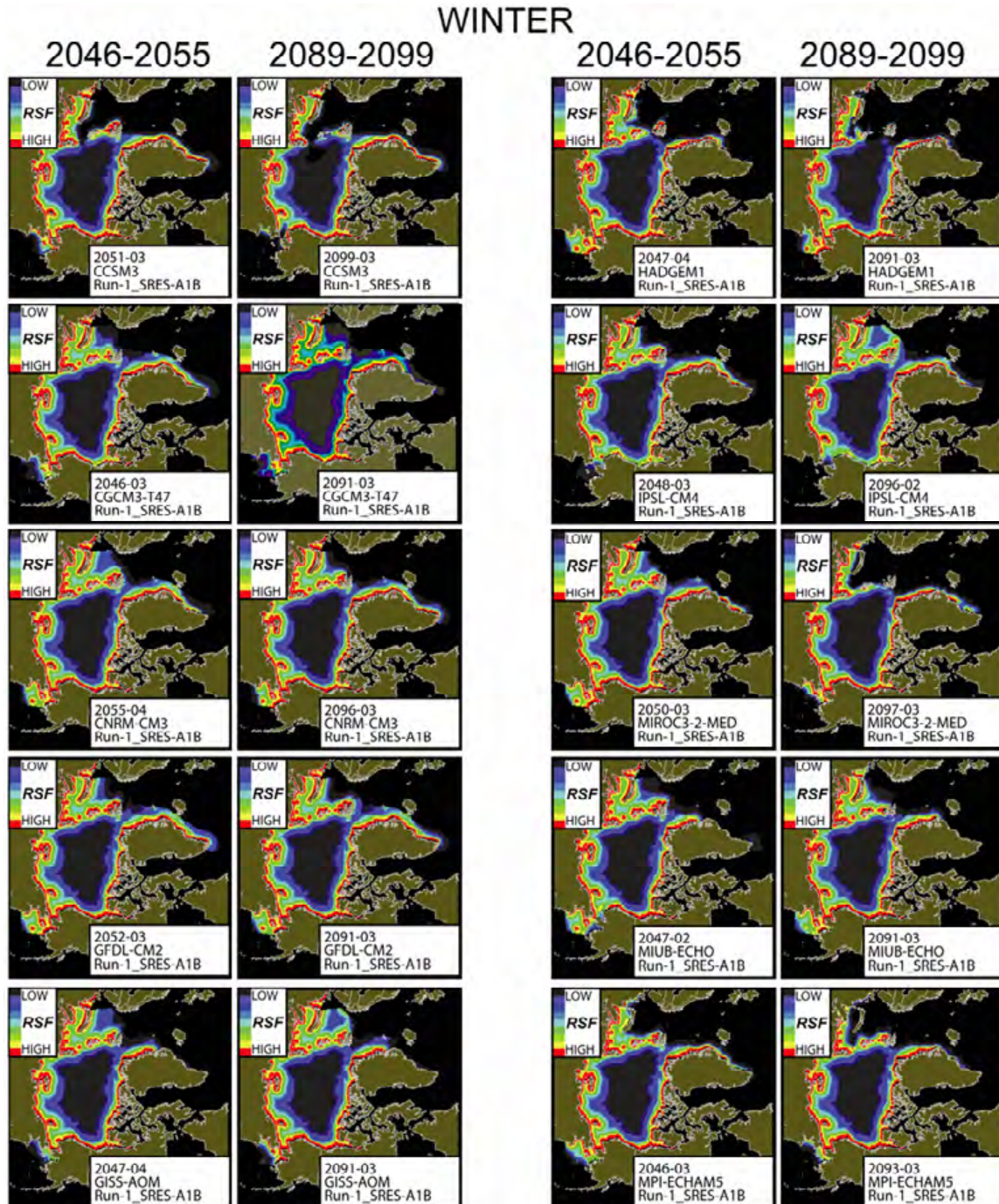
**Figure 10.** (a) Average monthly ice extent in the full study area during the summer and winter ice seasons (left column), and expressed as percent change (right column) relative to the respective model's 1990–1999 mean for the 20th century hindcasts and the satellite-observed record, and the 2001–2010 mean for the 21st century GCM projections. (b) Average monthly RSF habitat value (relative units of probability) summed throughout the study area during the summer and winter ice seasons (left column), and expressed as percent change (right column) relative to the decadal means defined above.

Average monthly values of ice extent (a, right column) during 1990–1999 from the satellite observed record are shown in brackets in the ice extent percent change panels to provide a baseline for assessing the effective magnitude of change. All results are plotted as 10-year running averages. Results for CCSM3 run under the B1 forcing scenario are shown with a dashed line.
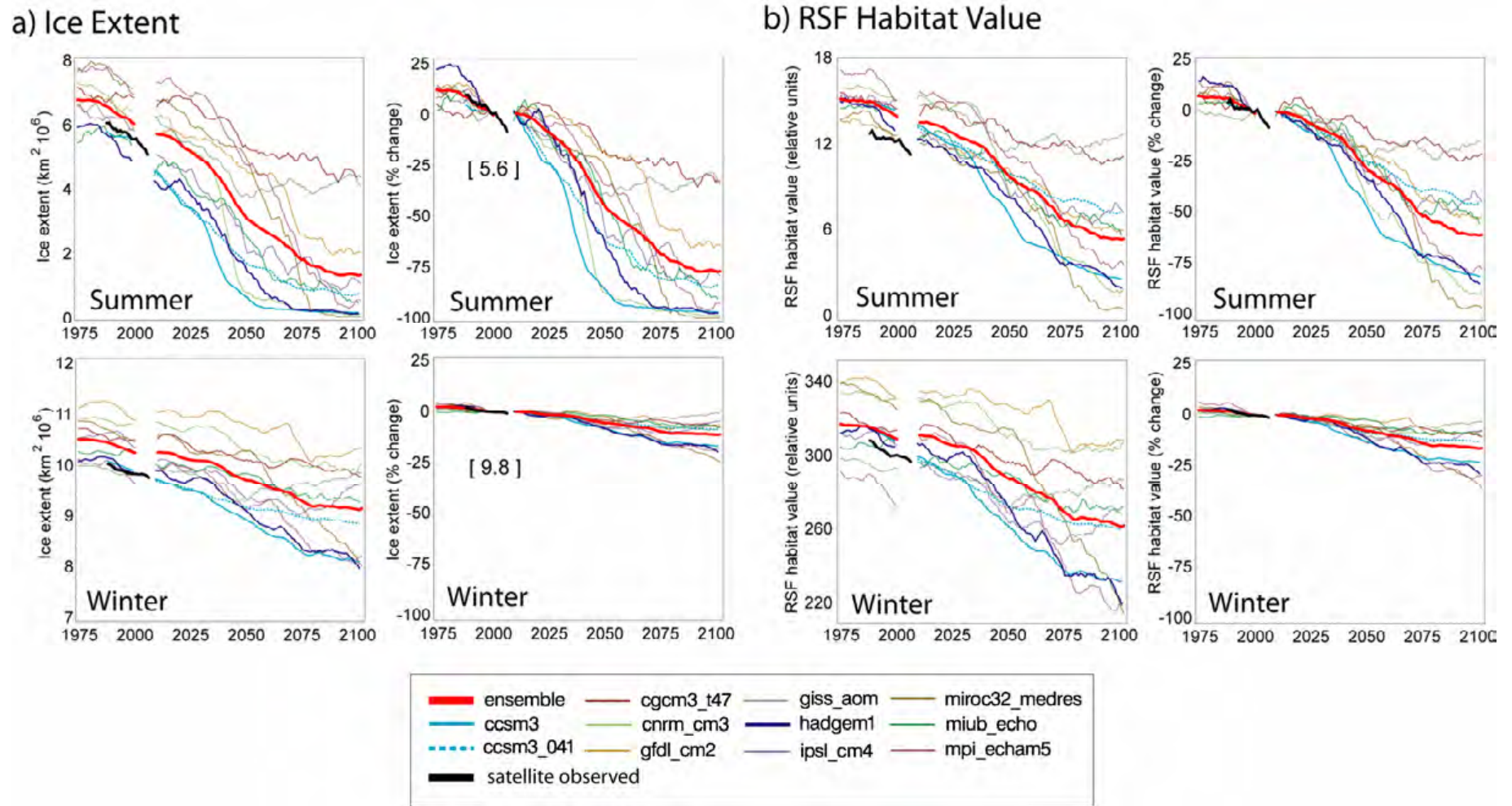
Figure 11a. Percent change in the total annual (Σ 12 months) area of optimal polar bear habitat in the IUCN units of the Alaska-Eurasia group, plotted as 10-year running averages. Results for CCSM3 run under the B1 forcing scenario are shown with a dashed line.

The average annual total area of optimal habitat (10^3 km^2) during 1990–1999 from the satellite observed record is shown in brackets to provide a baseline for assessing the effective magnitude of the percent change.

a) Alaska-Eurasia
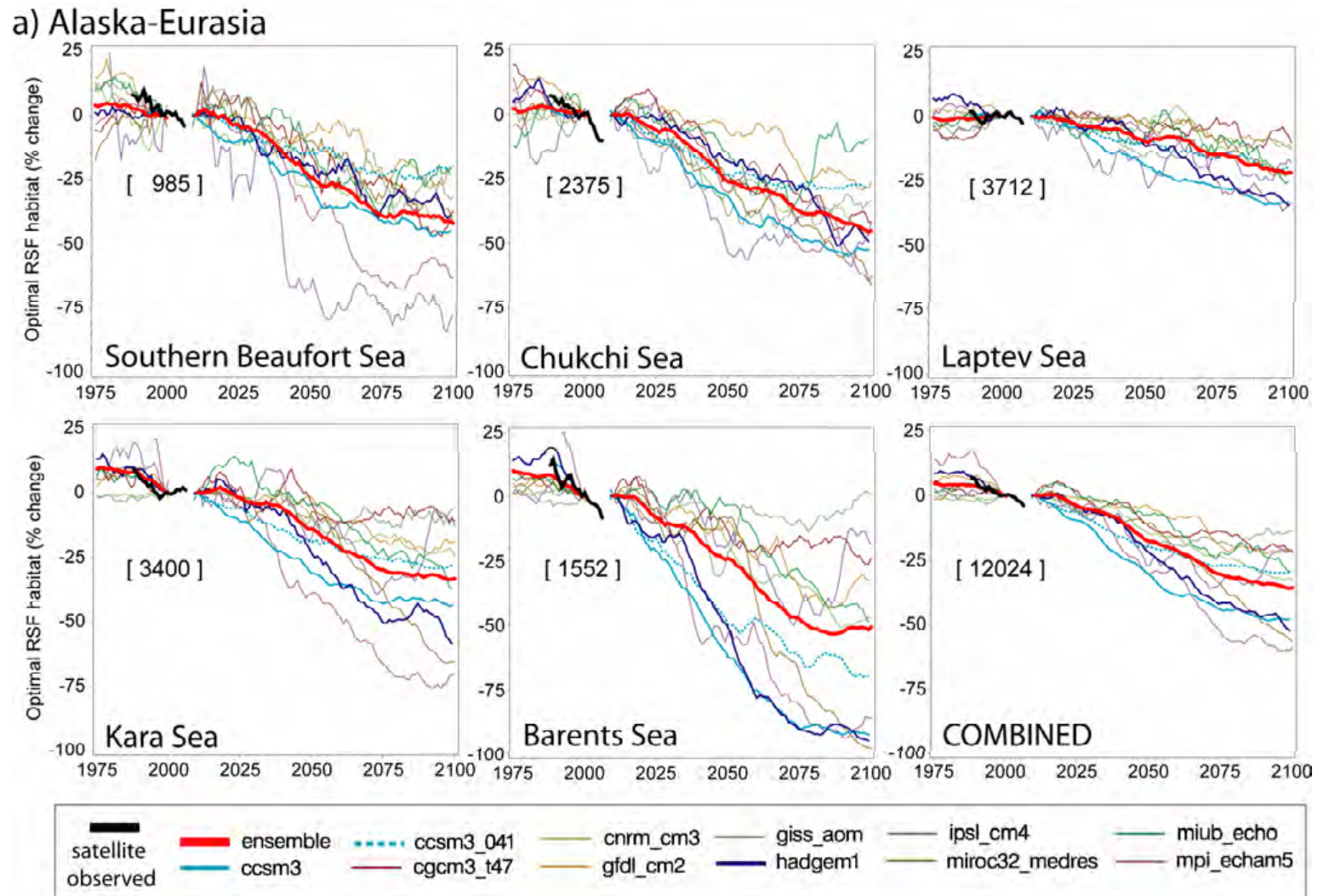
Figure 11b. Percent change in the total annual (Σ 12 months) area of optimal polar bear habitat in the IUCN units of the Canada-Greenland group, plotted as 10-year running averages. Results for CCSM3 run under the B1 forcing scenario are shown with a dashed line.

Note the y-axis is scaled different for the Arctic Basin unit. The average annual total area of optimal habitat (10^3 km^2) during 1990–1999 from the satellite observed record is shown in brackets to provide a baseline for assessing the effective magnitude of the percent change.
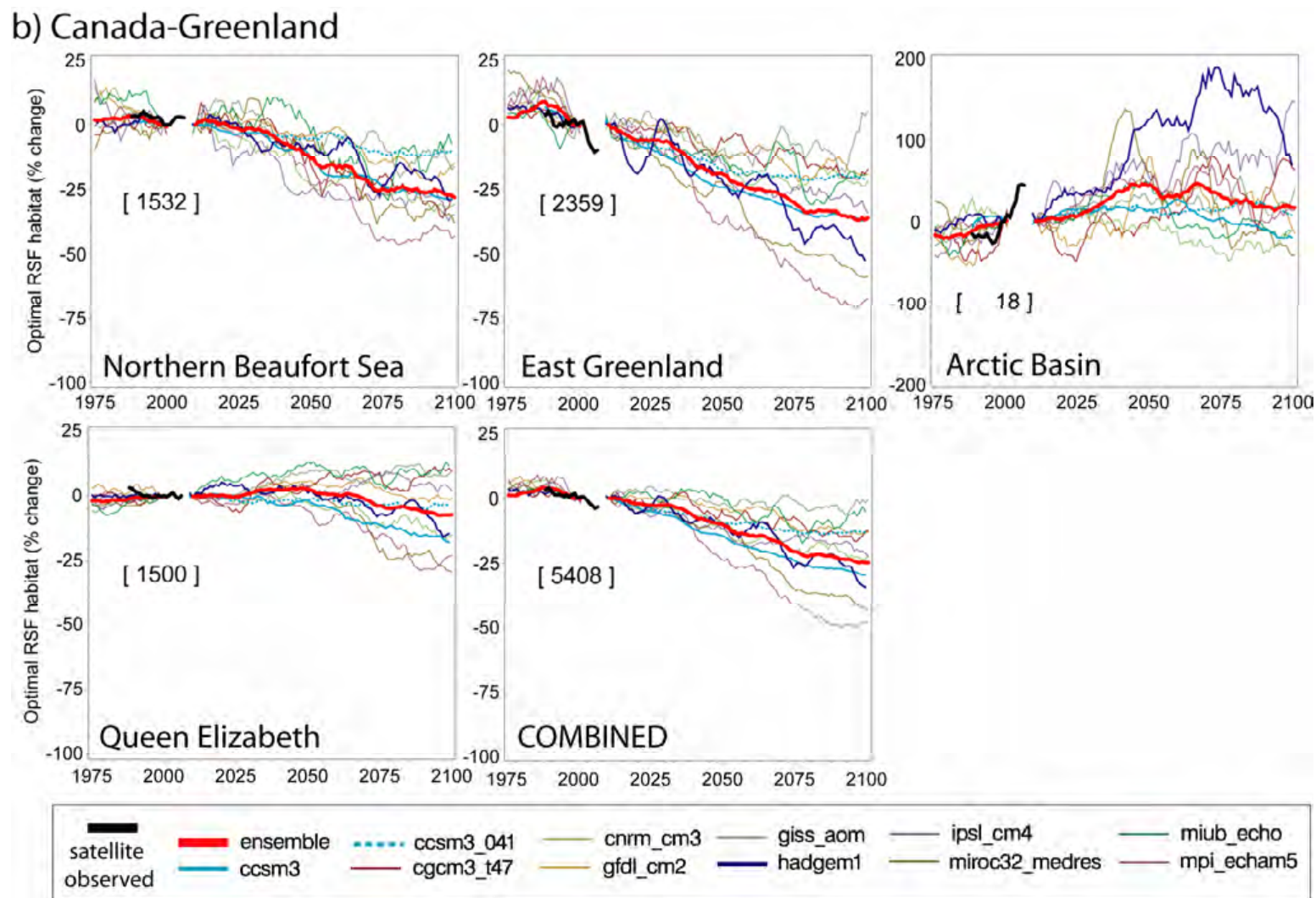
b) Canada-Greenland

Figure 12. (upper histograms) Mean area of optimal polar bear habitat in the (a) full study area, (b) Alaska-Eurasia IUCN group, and (c) Canada-Greenland IUCN group, during 2 decadal periods of the satellite observed sea ice record, and 3 decadal periods of the 21st century based on sea ice projections by 10 IPCC AR-4 GCMs (ensemble mean with 1 std error) for each of 4 ice seasons and annually; (lower histograms) the corresponding within-season percent change in optimal habitat area relative to the first (1985–1995) decadal period.
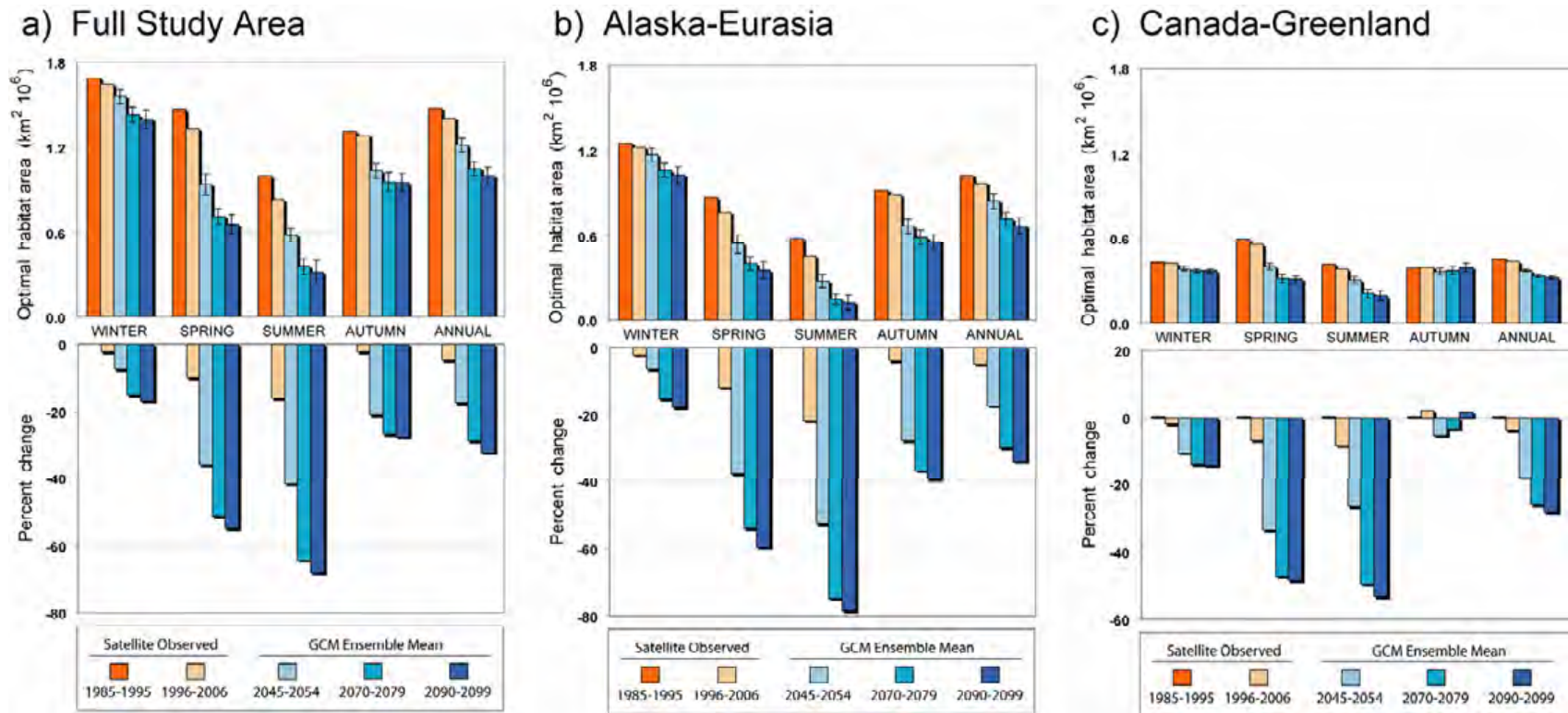
Figure 13. Observed changes in the spatial distribution and integrated annual area of optimal polar bear habitat.

Base map shows the cumulative number of months per decadal period where optimal polar bear habitat was either lost (red) or gained (blue) from 1985–1995 to 1996–2006. Offshore gray shading denotes areas where optimal habitat was absent in both periods. Insets show the average annual (Σ 12 months) cumulative area of optimal habitat (right y-axis, line plot) for the two 11-year periods (x-axis), and their associated percent change in area (left y-axis, histograms) relative to the first period (1985–1995).
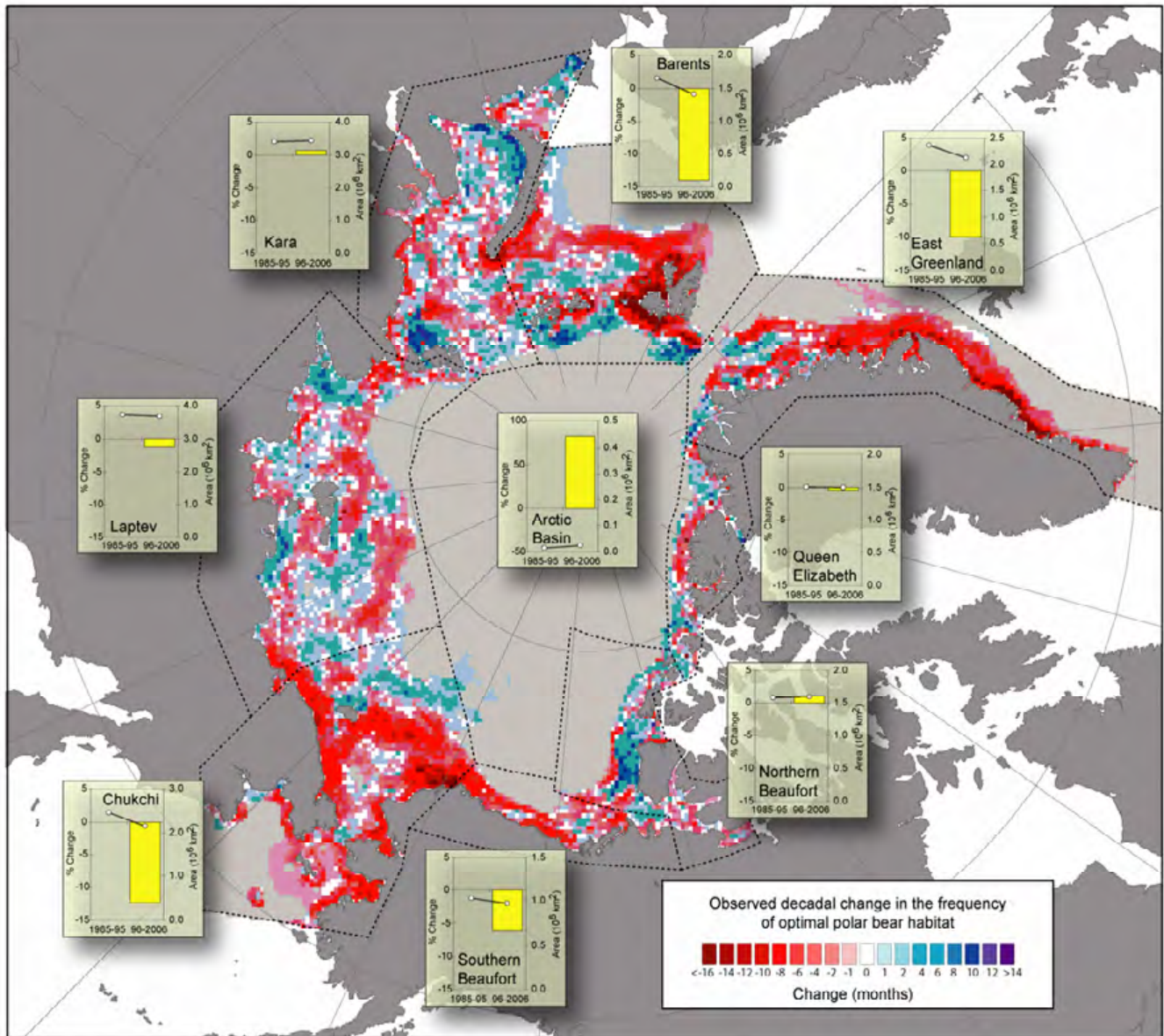
Figure 14. Projected changes (based on 10 IPCC AR-4 GCM models run with the SRES-A1B forcing scenario) in the spatial distribution and integrated annual area of optimal polar bear habitat.

Base map shows the cumulative number of months per decade where optimal polar bear habitat was either lost (red) or gained (blue) from 2001–2010 to 2041–2050. Offshore gray shading denotes areas where optimal habitat was absent in both periods. Insets show the average annual (Σ 12 months) cumulative area of optimal habitat (right y-axis, line plot) for four 10-year periods in the 21st century (x-axis midpoints), and their associated percent change in area (left y axis, histograms) relative to the first decade (2001–2010).

Table A1. Coefficients, AIC values and AIC weights of winter resource selection functions.

Rank	Model	*totcon*	*totcon2*	*bath*	*dist2land*	*dist15*	*dist50*	*dist75*	AIC	AIC Weight
1	22	0.0860	-0.0005	-0.0004	-0.0047				48377.88	>0.999
2	7	0.0184		-0.0004	-0.0051				48405.12	<0.001
3	24	0.0967	-0.0005	-0.0004			-0.0036		48433.58	<0.001
4	23	0.1057	-0.0006	-0.0004		-0.0035			48438.94	<0.001
5	25	0.0837	-0.0005	-0.0004				-0.0034	48453.72	<0.001
6	9	0.0171		-0.0004			-0.0040		48470.61	<0.001
7	10	0.0140		-0.0004				-0.0038	48482.12	<0.001
8	8	0.0191		-0.0004		-0.0037			48486.62	<0.001
9	18	0.0769	-0.0004		-0.0068				48509.85	<0.001
10	3	0.0206			-0.0070				48529.07	<0.001
11	17	0.1213	-0.0007	-0.0006					48577.80	<0.001
12	20	0.0905	-0.0005				-0.0056		48623.38	<0.001
13	19	0.1044	-0.0006			-0.0054			48636.88	<0.001
14	2	0.0119		-0.0006					48652.52	<0.001
15	5	0.0194					-0.0059		48653.17	<0.001
16	21	0.0691	-0.0004					-0.0055	48653.55	<0.001
17	6	0.0150						-0.0058	48671.15	<0.001
18	4	0.0225				-0.0057			48681.56	<0.001
19	16	0.1311	-0.0008						49076.30	<0.001
20	1	0.0116							49171.69	<0.001

Table A2. Coefficients, AIC values and AIC weights of spring resource selection functions.

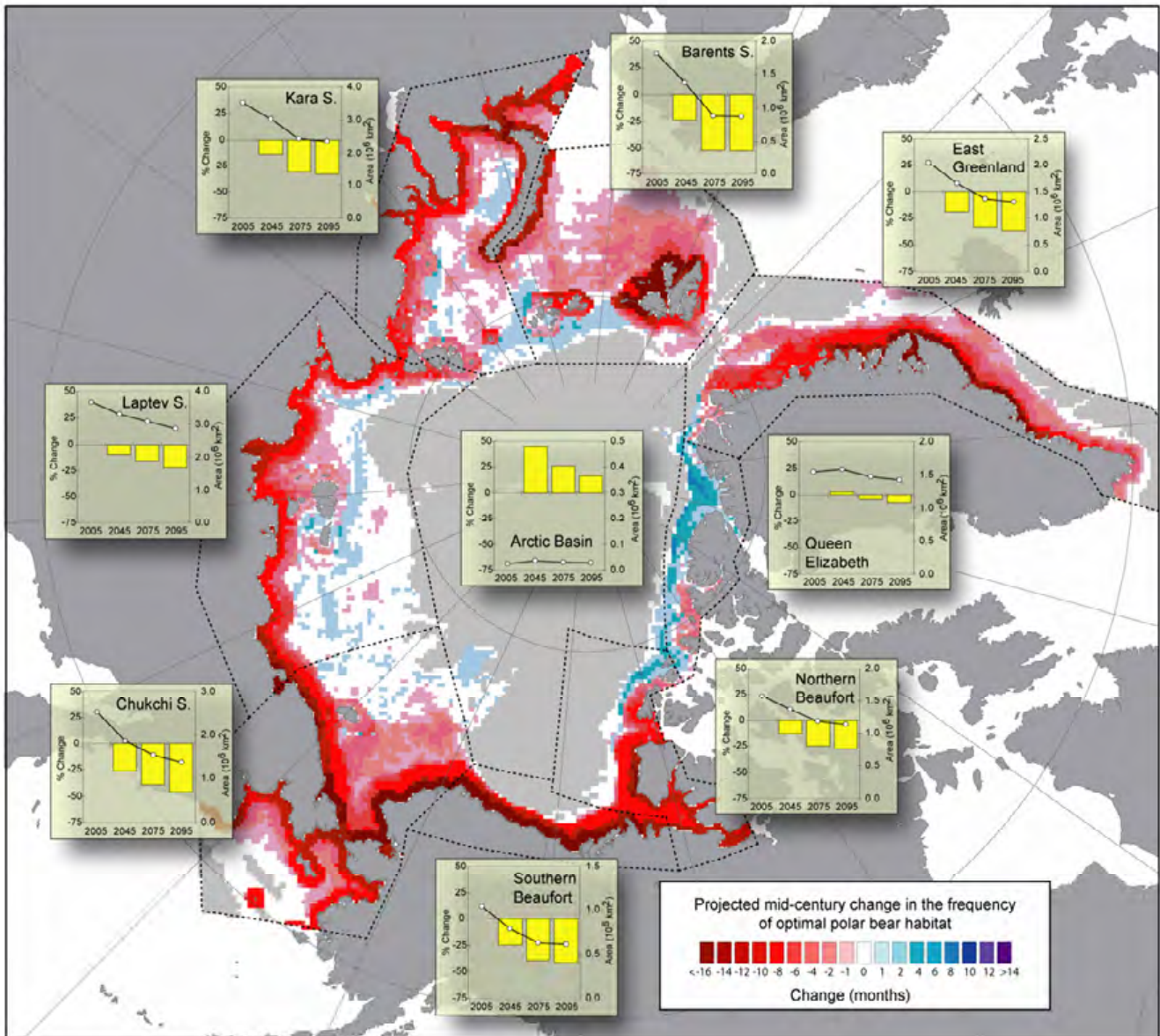| Rank	Model	*totcon*	*totcon2*	*bath*	*dist2land*	*dist15*	*dist50*	*dist75*	AIC	AIC Weight
1	23	0.0655	-0.0004	-0.0002		-0.0026			30646.72	>0.999
2	24	0.0552	-0.0003	-0.0002			-0.0022		30661.86	<0.001
3	25	0.0592	-0.0004	-0.0003				-0.0015	30673.69	<0.001
4	22	0.0662	-0.0004	-0.0002	-0.0014				30677.30	<0.001
5	19	0.0658	-0.0004			-0.0037			30685.75	<0.001
6	17	0.0673	-0.0005	-0.0003					30690.36	<0.001
7	26	0.0534	-0.0003		-0.0016		-0.0025		30699.64	<0.001
8	27	0.0572	-0.0004		-0.0024			-0.0017	30709.62	<0.001
9	29	0.0572	-0.0004		-0.0024			-0.0017	30709.62	<0.001
10	9	0.0201		-0.0002			-0.0038		30716.80	<0.001
11	20	0.0495	-0.0003				-0.0035		30717.32	<0.001
12	30	0.0487	-0.0003				-0.0032	-0.0004	30718.31	<0.001
13	18	0.0661	-0.0004		-0.0027				30730.96	<0.001
14	11	0.0199			-0.0013		-0.0040		30748.86	<0.001
15	8	0.0243		-0.0002		-0.0034			30749.33	<0.001
16	5	0.0188					-0.0047		30759.42	<0.001
17	15	0.0180					-0.0044	-0.0005	30759.93	<0.001
18	14	0.0208				-0.0038		-0.0019	30760.31	<0.001
19	21	0.0571	-0.0004					-0.0021	30764.38	<0.001
20	10	0.0157		-0.0003				-0.0027	30768.74	<0.001
21	4	0.0245				-0.0045			30787.45	<0.001
22	12	0.0163			-0.0027			-0.0027	30794.09	<0.001
23	16	0.0690	-0.0005						30801.36	<0.001
24	7	0.0210		-0.0002	-0.0020				30802.24	<0.001
25	2	0.0195		-0.0003					30831.47	<0.001
26	3	0.0204			-0.0033				30858.67	<0.001
27	6	0.0123						-0.0034	30864.57	<0.001
28	1	0.0166							30970.92	<0.001

Table A3. Coefficients, AIC values and AIC weights of summer resource selection functions.

Rank	Model	totcon	totcon2	bath	dist2land	dist15	dist50	dist75	AIC	AIC Weight
1	23	0.0468	-0.0004	-0.0002		-0.0044			15310.99	>0.999
2	19	0.0454	-0.0004			-0.0050			15330.76	<0.001
3	28	0.0483	-0.0004			-0.0053	0.0007		15331.54	<0.001
4	29	0.0465	-0.0004			-0.0050		0.0004	15332.09	<0.001
5	22	0.0538	-0.0005	-0.0002	-0.0026				15333.42	<0.001
6	26	0.0453	-0.0004		-0.0032		-0.0016		15342.55	<0.001
7	27	0.0505	-0.0005		-0.0034			-0.0009	15347.71	<0.001
8	18	0.0534	-0.0005		-0.0032				15349.40	<0.001
9	24	0.0437	-0.0004	-0.0002			-0.0020		15350.10	<0.001
10	8	0.0179		-0.0002		-0.0062			15360.54	<0.001
11	17	0.0540	-0.0005	-0.0002					15361.95	<0.001
12	25	0.0523	-0.0005	-0.0002				-0.0005	15362.63	<0.001
13	13	0.0145				-0.0061	-0.0011		15379.83	<0.001
14	4	0.0161				-0.0069			15381.52	<0.001
15	14	0.0162				-0.0069		0.0001	15383.51	<0.001
16	30	0.0444	-0.0004				-0.0024	0.0011	15391.57	<0.001
17	20	0.0445	-0.0005				-0.0017		15393.16	<0.001
18	11	0.0105			-0.0037		-0.0039		15393.39	<0.001
19	9	0.0082		-0.0003			-0.0044		15400.80	<0.001
20	16	0.0535	-0.0006						15401.03	<0.001
21	21	0.0531	-0.0006					-0.0001	15402.98	<0.001
22	7	0.0144		-0.0002	-0.0034				15437.48	<0.001
23	12	0.0097			-0.0045			-0.0019	15445.11	<0.001
24	15	0.0068					-0.0055	0.0020	15449.38	<0.001
25	5	0.0035					-0.0044		15459.18	<0.001
26	3	0.0127			-0.0041				15460.02	<0.001
27	10	0.0069		-0.0003				-0.0016	15480.58	<0.001
28	2	0.0096		-0.0003					15489.77	<0.001
29	6	0.0026						-0.0012	15546.61	<0.001
30	1	0.0048							15551.60	<0.001

Table A4. Coefficients, AIC values and AIC weights of autumn resource selection functions.

Rank	Model	*totcon*	*totcon2*	*bath*	*dist2land*	*dist15*	*dist50*	*dist75*	AIC	AIC Weight
1	23	0.0813	-0.0007	-0.0002		-0.0060			15507.25	>0.999
2	19	0.0828	-0.0007			-0.0072			15540.11	<0.001
3	24	0.0508	-0.0004	-0.0003			-0.0061		15556.15	<0.001
4	22	0.0816	-0.0007	-0.0003	-0.0046				15568.22	<0.001
5	27	0.0699	-0.0006		-0.0053			-0.0022	15597.58	<0.001
6	29	0.0699	-0.0006		-0.0053			-0.0022	15597.58	<0.001
7	9	0.0044		-0.0003			-0.0082		15600.25	<0.001
8	18	0.0824	-0.0007		-0.0059				15612.92	<0.001
9	20	0.0443	-0.0004				-0.0077		15615.81	<0.001
10	25	0.0694	-0.0007	-0.0004				-0.0031	15636.93	<0.001
11	5	0.0025					-0.0095		15651.20	<0.001
12	8	0.0105		-0.0003		-0.0072			15655.38	<0.001
13	14	0.0044				-0.0071		-0.0030	15668.48	<0.001
14	17	0.0883	-0.0008	-0.0005					15671.33	<0.001
15	4	0.0101				-0.0085			15695.93	<0.001
16	12	-0.0021			-0.0055			-0.0043	15722.11	<0.001
17	7	0.0065		-0.0003	-0.0056				15738.86	<0.001
18	21	0.0647	-0.0007					-0.0046	15740.53	<0.001
19	10	-0.0060		-0.0004				-0.0055	15772.62	<0.001
20	3	0.0052			-0.0071				15792.83	<0.001
21	16	0.0947	-0.0009						15827.97	<0.001
22	6	-0.0117						-0.0071	15879.06	<0.001
23	2	0.0015		-0.0005					15905.63	<0.001
24	1	-0.0038							16134.16	<0.001